

1
2
3
4
5
6
7
8
9
10
11
12
13
14
15

**On the structural diversity and individuality of
polymorphic amyloid protein assemblies**

Liisa Lutter, Liam D. Aubrey, Wei-Feng Xue*

School of Biosciences, Division of Natural Sciences, University of Kent, CT2 7NJ,
Canterbury, UK

* Correspondence to: W.F.Xue@kent.ac.uk; Tel +44-(0)1227 824821

1 **Abstract**

2

3 The prediction of highly ordered three-dimensional structures of amyloid protein fibrils from
4 the amino acid sequences of their monomeric self-assembly precursors constitutes a
5 challenging and unresolved aspect of the classical protein folding problem. Because of the
6 polymorphic nature of amyloid assembly whereby polypeptide chains of identical amino acid
7 sequences under identical conditions are capable of self-assembly into a spectrum of different
8 fibril structures, the prediction of amyloid structures from an amino acid sequence requires a
9 detailed and holistic understanding of its assembly free energy landscape. The full extent of
10 the structure space accessible to the cross- β molecular architecture of amyloid must also be
11 resolved. Here, we review the current understanding of the diversity and the individuality of
12 amyloid structures, and how the polymorphic landscape of amyloid links to biology and disease
13 phenotypes. We present a comprehensive review of structural models of amyloid fibrils derived
14 by cryo-EM, ssNMR and AFM to date, and discuss the challenges ahead for resolving the
15 structural basis and the biological consequences of polymorphic amyloid assemblies.

16

17

18

1 **Research Highlights**

2

3 • Amyloid structures are highly polymorphic in that the folding/misfolding-assembly of
4 a single polypeptide sequence into the amyloid state may result in many different fibril
5 structures.

6 • Prediction of amyloid structures from a primary amino acid sequence is a ‘one sequence
7 to many structures’ problem due to polymorphism, and this challenge is far from being
8 resolved.

9 • Structural data of amyloid in the PDB and the EMDB released to date (up to March
10 2021) show considerable presence of polymorphism, and are summarised in this review.

11 • Cryo-EM and ssNMR have revealed extensive diversity of amyloid structures that all
12 share the defining cross- β fibril core architecture of amyloid.

13 • AFM has revealed the individuality displayed by each fibril structure in heterogeneous
14 amyloid populations.

15

1 List of Abbreviations

2

3 3D – three-dimensional

4 Å – ångström

5 AD – Alzheimer’s disease

6 AFM – atomic force microscopy

7 AI – artificial intelligence

8 AL – amyloid light chain

9 A β_{40} – amyloid β peptide fragment, amino acid residues 1-40

10 A β_{42} – amyloid β protein fragment, amino acid residues 1-42

11 CASP – Critical Assessment of protein Structure Prediction

12 CASP14 – 14th Community Wide Experiment on the Critical Assessment of Techniques for

13 Protein Structure Prediction

14 CBD – corticobasal degeneration

15 Cryo-EM – cryogenic electron microscopy

16 dGAE – tau protein fragment, amino acid residues 297-391

17 EM – electron microscopy

18 EMDB – The Electron Microscopy Data Bank

19 IAPP – islet amyloid polypeptide

20 microED – microcrystal electron diffraction

21 PDB – The Protein Data Bank

22 PTMs – post-translational modifications

23 RCSB – Research Collaboratory for Structural Bioinformatics

24 ssNMR – solid-state nuclear magnetic resonance

1 Introduction

2

3 Amyloid structures represent a class of filamentous protein self-assemblies that are defined by
4 their characteristic core structures containing β -strands arranged perpendicularly to the fibril
5 axis [1,2]. This highly ordered three-dimensional (3D) structural arrangement, called the cross-
6 β architecture, confers amyloid fibrils with high chemical, mechanical and biological stability,
7 in part due to the network of hydrogen bonds running between the β -sheets present throughout
8 the fibrils, parallel to the fibril axis. Deposits of amyloid are associated with pathology in more
9 than 50 human disorders, including neurodegenerative diseases as well as type 2 diabetes, prion
10 diseases and systemic amyloidoses [3]. Some amyloid proteins, however, form fibrils required
11 for physiological functionalities [4]. In humans, more than 20 proteins have been shown to
12 form amyloid, despite having vastly different amino acid sequences [5]. The assembly into the
13 amyloid state proceeds through a nucleated polymerisation mechanism in which natively
14 folded or intrinsically disordered protein monomers unfold or misfold, and aggregate into
15 dynamic and transient oligomers [6]. Some of these species go through primary nucleation
16 events to form nuclei, which are the smallest units from which growth of aggregates by
17 energetically favourable elongation into fibrils can proceed by monomer addition to fibril ends
18 [7,8]. The resulting amyloid state self-propagates by catalysis of new nucleation events by
19 existing fibril surfaces, and through fibril fragmentation, which produces seeds by division of
20 the fibrils without undergoing an additional nucleation phase [9,10].

21

22 Compared to the folding reaction of globular proteins, amyloid formation stands out because
23 it possesses unique properties. Firstly, the coupled folding-assembly reaction of monomeric
24 peptide chains into the amyloid state occurs as a result of intermolecular interactions between
25 a large but variable number of monomers. Secondly, the resulting protein conformations of

1 amyloid fibrils are capable of self-propagation. This property allows the information encoded
2 in the individual 3D structures of amyloid and prions, which represent a class of infectious
3 amyloid that can spread between individual organisms [11], to be transmitted to monomers not
4 yet in the amyloid state. Thirdly, although the end-products of a single type of amyloid
5 assembly reaction are fibrils sharing the defining cross- β core architecture, there may be a wide
6 degree of variation between their specific structures, even when the assembly reactions start
7 with identical monomeric polypeptide chains under identical conditions. This property, called
8 structural polymorphism, is biologically important because it affects the physicochemical
9 properties of the fibrils, which subsequently may reflect the variation in the biological response
10 to amyloid *in vivo*. For example, specific amyloid polymorphs formed from the same tau
11 protein are found in different tauopathies [12], and within each disease-specific amyloid
12 population there can exist several types of polymorphic fibrils [13–15]. However, structural
13 polymorphism complicates any attempt of predicting a protein's 3D shape from its amino acid
14 sequence, because in the case of amyloid, one single amino acid sequence may fold/misfold
15 and assemble into a spectrum of different 3D structures.

16

17 Experimental techniques that have been applied to study the polymorphous amyloid structures
18 include cryo-electron microscopy (cryo-EM), solid-state nuclear magnetic resonance (ssNMR)
19 spectroscopy, and atomic force microscopy (AFM) (**Table 1**). Methodological advances in
20 Cryo-EM has, in recent years, led to the elucidation of numerous structural models of amyloid
21 fibrils [16]. These cryo-EM derived models are made with 3D Coulomb potential maps,
22 reconstructed nowadays routinely to sub-4 Å resolutions, using 2D projection images of
23 fibrillar samples collected on modern cryo-EM microscopes. For ssNMR, spectroscopic data
24 of nuclear resonance frequencies are collected on fibril samples formed from isotopically
25 labelled protein monomers. The interpretation of the resulting chemical shifts and atomic

1 distance constraints are used to reconstruct an ensemble of possible conformations of each
2 single structural model [17]. AFM allows the morphologies of individual fibrils to be directly
3 visualised on 2D topology images to a low-nanometre resolution, from which 3D envelope
4 models of each individually observed fibril can then be reconstructed [18]. Combining AFM
5 with infrared spectroscopy (AFM-IR) [19] or Raman spectroscopy (AFM-Raman) [20], allows
6 the secondary structure content of individual fibrils or aggregates to also be assessed. The 3D
7 structural models obtained by these techniques, and the subsequently observed structural
8 polymorphism, are discussed in this review.

9
10 Recently, advance in the prediction of protein structures from their primary sequences by
11 AlphaFold 2, a machine learning-based method developed by Google's DeepMind AI research
12 group, showed that its structural predictions can now nearly match experimental results [21].
13 This was demonstrated by participation in the 14th Community Wide Experiment on the
14 Critical Assessment of Techniques for Protein Structure Prediction (CASP14), a biennial
15 community experiment in which international research teams participate to evaluate the
16 accuracy of their protein structure prediction methods (e.g. [22,23]). Despite this important
17 advance, AlphaFold 2 has not yet been applied to multimeric protein structure prediction [21],
18 even though accurate prediction of multi-protein complex structures such as amyloid fibrils
19 could revolutionise aspects of key applications, including drug design. This highlights the
20 magnitude of unresolved challenges in structural prediction of large protein assemblies, and
21 the need to establish a fundamental understanding between amino acid sequence, amyloid
22 structure, function, and pathogenicity. Thus, predicting the 3D structures of polymorphic
23 amyloid fibrils from primary amino acid sequences is exceptionally challenging, but also offers
24 important opportunities for contributing to our fundamental understanding of coupled protein
25 folding and assembly free energy landscapes, as well as for potentially important applications

1 in the development of anti-amyloid drugs for neurodegenerative diseases. This challenge can
2 only begin to be addressed through the characterisation of the extent of amyloid polymorphism
3 as well as the individual 3D structures of polymorphs formed. Here, we review recent advances
4 in our understanding of amyloid polymorphism through recent structural data that reveal the
5 diversity of amyloid fibril structures that can be formed, and the individuality of filament
6 structures that exists within heterogeneous amyloid populations. We discuss the resulting
7 physicochemical and biological consequences of amyloid polymorphism, the challenges of
8 amyloid structure prediction, and opportunities where such contributions could provide new
9 fundamental insights or applications.

10

11

12 **The paradox of amyloid polymorphism: from one amino-acid** 13 **sequence to many three-dimensional structures**

14

15 Recent studies of the 3D structures of amyloid fibrils have revealed extensive presence of
16 structural polymorphism in high-resolution detail. Different, but ordered and stable amyloid
17 structures have been shown to assemble from polypeptide chains of the same primary amino
18 acid sequence. This contradicts the uniqueness condition of Anfinsen's dogma stating that a
19 uniquely dominating energy minimum in the free energy landscape of a polypeptide chain is
20 required for it to fold into a unique native 3D structure [24]. Instead, it appears that the free
21 energy landscape for amyloid protein folding/misfolding and assembly consists of many local
22 minima of similar levels of free energy, and the extent of such local minima groups are affected
23 by factors that include the primary amino acid sequence of the monomeric building blocks of
24 the fibrils [25]. This structural polymorphism creates a considerable challenge for 3D structure
25 prediction from primary sequence as one sequence can result in many different stably

1 observable structures. Importantly, the structural polymorphs observed to date do not only
2 result from different contacts between residues in the fibril cores that then lead to different
3 overall folds, but instead involves a number of possible variations which interplay in a
4 hierarchical manner [26,27] (**Fig. 1**). Firstly, different amyloid structures may result from ‘top-
5 level’ modifications in the primary amino acid sequence such as point-mutations,
6 truncations/deletions and/or post-translational modifications (top row of **Fig. 1**). However,
7 these ‘top-level’ modifications involve changes in the covalent bonding pattern and can be
8 classified as sequence polymorphism rather than structural polymorphism, and thus do not
9 wholly reflect the complexities of amyloid sequence-structure relationships. Secondly, further
10 complexities arise from the conformational arrangements of protofilaments, which are
11 filamentous building blocks that make up the fibril structures. In the protofilament core, the
12 extent and the packing of β -sheet- and random coil-forming regions, as well as disordered
13 regions, often vary even for monomeric polypeptide chains of identical sequences. Co-factors
14 in the fibril core may also be necessary for stabilising specific folds, further contributing to
15 structural polymorphism. There are also known instances where protofilaments are formed by
16 multiple different polypeptide sequences, thus resulting in heteroamyloid fibrils (second row
17 of **Fig. 1**). Thirdly, although conformational differences in the protofilament core formed from
18 a single amyloid protein or peptide sequence can display remarkable structural diversity, it is
19 also common for amyloid fibrils to assemble and form structures involving multiple
20 protofilaments (third row of **Fig. 1**). In this case, each monomeric layer of the fibril consists of
21 multiple copies of the same peptide chain, which can be arranged in a number of different ways.
22 Notably, the protofilament building blocks of amyloid fibrils can have identical or different
23 folds, and their lateral arrangement can vary. Finally, structural polymorphism can also arise
24 from variations in the fibrils’ mesoscopic (nm to μ m length-scale) arrangements like twist
25 handedness, twist pitch, the position of the fibril screw-axis, and fibril length. These long-range

1 properties contribute to the molecular individuality of amyloid fibrils, which may subsequently
2 also impact the biological response the fibrils elicit.
3
4 Due to polymorphic folding and assembly landscapes, the prediction of amyloid structures
5 from their constituent monomeric amino acid sequences is challenging. The hierarchical nature
6 of structural polymorphism, which has been experimentally observed to give rise to many
7 diverse structures from identical protein sequences, may lead to a continuous cloud of
8 polymorphs within a population of amyloid fibrils, with individual fibrils populating the
9 structure space defined by local energy minima with differing probabilities. Thus, the
10 possibility of diverse and individualistic amyloid structures resulting from the
11 folding/misfolding-assembly of identical polypeptide chains presents a conundrum in terms of
12 whether the cloud of structures formed also translates into equally diverse biological or
13 phenotypical responses, and whether it is possible to predict amyloid structures and subsequent
14 function with some degree of certainty. It is currently not possible to assess how well structural
15 prediction tools would predict amyloid structures as none have yet been included as CASP
16 targets. However, structural prediction of multimeric CASP targets is a greater challenge
17 compared to monomeric targets due to the necessity of predicting how multiple monomeric
18 subunits interface with each other [28]. Therefore, prediction of amyloid fibril structures,
19 which have multiple interfacing monomeric subunits and, in addition, exhibit a wide degree of
20 polymorphism (see **Fig. 1**), will require significant additional advances to current methods.
21 Current prediction tools specifically designed for amyloid sequences are focused on predicting
22 the amyloid forming propensity of sequence regions, with some offering additional predictions
23 of intrinsic disorder and secondary structure (e.g. [29–31]). Nevertheless, predicting the
24 amyloidogenic regions and aggregation propensity has been challenging even for short
25 peptides [32,33].

1
2
3
4
5
6
7
8
9
10
11
12
13
14
15
16
17
18
19
20
21
22
23
24
25

The structural diversity of filamentous amyloid assemblies

Amyloid fibrils are defined by a characteristic cross- β structure formed by β -strands with 4.7 Å spacing, stabilised by a hydrogen bonding network parallel to the fibril axis, and tight side-chain packing between two β -sheets with 10 Å spacing. This cross- β architecture can be experimentally readily observed in X-ray fibre diffraction patterns [34]. Importantly, the 3D structures of a growing number of amyloid fibrils have been experimentally resolved in the last five years, revealing extensive presence of structural polymorphism (see **Table 2** and **Fig. 2** for a summary of structural data in the EMDB and the PDB released up until March 2021).

The elucidation of amyloid 3D structures in atomic detail was pioneered by X-ray diffraction experiments of amyloid peptide microcrystals, allowing the variation in the β -sheet arrangements to be experimentally characterised and the features that stabilise the cross- β fold to be studied [35]. This revealed, for example, the tight inter-digitating side chains that make up the dry interface between β -sheets, termed steric zippers, and the hydrogen-bonding ladders formed by stacking of specific side-chains along the length of the long fibril axis. Eight different possible classes of steric zippers have been described, with differences arising from the parallel or antiparallel direction of the β -sheets, and the relative orientations of the two connecting β -sheets [35]. More recently, microcrystal electron diffraction (microED) has been employed to elucidate the structures of amyloid peptide crystals, with the advantage that even nano-sized crystals too small for conventional X-ray crystallography experiments can be amenable for analysis [36]. Formation of crystals for structural studies is, however, limited by the length of the amyloid forming peptide. Therefore, amyloid structures formed from larger

1 polypeptide fragments or full-length proteins have been mainly resolved using solid state
2 nuclear magnetic resonance spectroscopy and cryo-electron microscopy. Although ssNMR has
3 been used to generate structural models of amyloid fibrils for nearly two decades, it was the
4 ‘resolution revolution’ of cryo-EM that led to the increased rate in the number of data entries
5 of amyloid fibrils deposited to the EMDB and PDB databases in recent years. The average
6 resolution of cryo-EM maps has also markedly improved in the last five years (**Fig. 3**).
7 Advances in cryo-EM hardware and increased accessibility to equipment have driven the
8 collection of evermore number of high-quality datasets of amyloid fibril samples, whereas
9 improved software for helical reconstruction and refinement have facilitated 3D reconstruction
10 with resolutions that regularly allow *de novo* building of molecular models [37]. These recent
11 advances have made possible the wide-ranging characterisation of amyloid fibril structures and
12 the types of polymorphic features they exhibit in detail, revealing the diversity in the
13 conformation of the fibril cores, the possible presence of post-translational modifications
14 (PTMs) and co-factors, the span of cross- β forming regions, and the extent of ordered and
15 dynamic regions within amyloid fibrils. Here, structural models of amyloid fibrils determined
16 by cryo-EM and ssNMR available in the EMDB and PDB databases up to March 2021 are
17 listed in **Table 2** and correspondingly visualised in **Figure 2** to both illustrate the diversity of
18 cross- β structures as well as provide an organised resource that facilitates comparison.

19

20 The evermore detailed information on amyloid fibril core structures has revealed a large degree
21 of polymorphism, which can be classified in a hierarchical manner as illustrated in **Figure 1**.
22 Especially interesting are polymorphic structures formed from protein chains with an identical
23 sequence, which exhibit fibril polymorphism in protofilament folds, filament assemblies, and
24 mesoscopic properties, as these features indicate sensitivity of the assembly process to
25 environmental conditions in determining the extent of polymorphism and the individuality of

1 the formed fibril structures. For example, amyloid fibrils formed from A β ₄₀ and A β ₄₂ result in
2 considerably different structures with different protofilament folds and assemblies (see **Fig. 2**,
3 entries 1 to 24, and **Table 2** for accession codes), likely due to the different conditions in which
4 the fibrils were formed. Structures of the same protein with different disease-associated
5 mutations and post-translational modifications have also been shown to form structures with
6 different morphologies. For example, structural data are available for α -synuclein with three
7 different mutations related to early-onset Parkinson's disease, E46K, A53T, and H50Q (see
8 **Fig. 2** and **Table 2**, entries 33, 34, 35, 41 and 42). Comparing the structures and their properties,
9 such as stability and seeding propensity, to those of wild-type fibrils may indicate how
10 polymorphism varies between familial and sporadic cases. Recently a combined cryo-EM and
11 mass spectrometry approach has also revealed specific PTMs on tau fibrils from *ex vivo* patient
12 brain tissue (see **Fig. 2** and **Table 2**, entries 97-99) [38]. Identification of disease-relevant
13 modifications is crucial for understanding how PTMs may modulate fibril polymorphism and
14 its biological effects. Importantly, the current structural data have shown differences between
15 fibril structures extracted from *ex vivo* tissues and those assembled *in vitro* from recombinant
16 protein monomers (e.g. see **Fig. 2** and **Table 2** entries 92-95) [39]. This is indicative of the
17 importance and the challenge of studying amyloid polymorphism in disease contexts in order
18 to understand possible disease-relevant sequence modifications and local *in vivo* environmental
19 factors. Additionally, it was recently shown that seeded formation of amyloid using fresh
20 monomer incubated with *ex vivo* fibril seeds does not necessarily replicate the structure of the
21 seed in the case of α -synuclein from multiple system atrophy patient brain tissue [40]. It is
22 currently not known if seeding may not propagate fibril structures due to a non-matched PTM
23 pattern of the monomer compared to that of the seeds, if co-factors that may be present in the
24 fibril core are missing in the seeded reactions, or if the assembly conditions during seeding are
25 too different to those during the formation of the seeds in general. It is also unclear how this

1 may vary for different amyloid systems that exhibit different kinetic rates for templated
2 elongation and secondary nucleation [41]. Nevertheless, these results demonstrate that
3 structures of fibrils formed from seeded growth using *ex vivo* fibril seeds should not necessarily
4 be assumed to be identical to those of the patient derived seeds without further evidence [42,43],
5 due to the complexities arising from the polymorphism-prone nature of amyloid. In summary,
6 detailed structural characterisation of amyloid fibrils, enabled by methodological advances in
7 cryo-EM and ssNMR, has demonstrated a remarkable tendency for many amyloid forming
8 polypeptide sequences to each form a diverse range of polymorphic cross- β amyloid structures.

9

10

11 **The individuality of amyloid structures**

12

13 The potential of amyloid fibrils to display a diverse range of cross- β structures (**Fig. 2**) due to
14 polymorphism resulting from the vast number and combinations of possible arrangements of
15 the polypeptide chains within each fibril (**Fig. 1**) means that the structures of amyloid fibrils
16 should also be considered with respect to individual fibrils. Each individual fibril in a
17 heterogeneous amyloid population may be distinguishable from every other fibril in the same
18 population in terms of its precise structure, stability, and biological properties, even when the
19 primary sequence of the monomeric polypeptide chains making up the fibrils is the same. This
20 is because many of the possible structural variations which underpin the observed amyloid
21 polymorphism are based on differences in the pattern of the energetically weak non-covalent
22 interactions (rows 2, 3 and 4 in **Fig. 1**), especially those peripheral to the cross- β protofilament
23 core (rows 3 and 4 in **Fig. 1**). Experimental observations by negative-stain electron microscopy
24 and atomic force microscopy (AFM) have shown that amyloid fibril populations can be highly
25 heterogeneous [44–48]. Advances in AFM imaging over the last two decades have contributed

1 with the discovery that the differences between structural polymorphs of amyloid, such as the
2 number of protofilaments, twist patterns, and the thickness of fibrils, which are all influenced
3 by the structure of the amyloid core, can indeed vary from fibril to fibril within a population
4 [25,46,48,49].

5

6 Modern AFM imaging methods can detect and characterise the structures of individual amyloid
7 fibrils within complex and heterogeneous samples. While the imaging resolution achievable
8 by AFM in one of the three spatial dimensions, i.e., the z- or height-axis, can now routinely
9 reach sub-ångströms under ambient conditions, the overall 3D-resolution of AFM has not yet
10 reached that currently achievable by cryo-EM. However, due to its underlying high signal-to-
11 noise physics, the structures of individual particles of amyloid can be characterised to ~nm
12 resolution without the extensive cross-particle averaging that cryo-EM methodologies rely on.
13 Recently, we have developed a method to reconstruct the 3D surface envelopes of individual
14 helical amyloid fibrils using the 3D information encoded in AFM height topology images [18]
15 (**Fig. 4**). This advance, combined with a systematic morphometric analysis and classification
16 of individually reconstructed 3D fibril models, enables the detection and structural
17 characterisation of individual, potentially rare, amyloid fibril species, and structural variations
18 within individual fibrils. The heterogeneity of a polymorphic amyloid population can also be
19 quantitatively assessed using AFM data by analysing the variations in fibril width, cross-
20 sectional area and shape, twist periodicity and twist handedness of individual fibrils within the
21 population. We demonstrated the potential of this approach to map the assembly landscapes of
22 amyloid by analysis of amyloid fibrils formed from three different peptide sequences (**Fig. 4**
23 left column and **Fig. 5**). The assembly landscape of these peptides show amino acid sequence
24 dependent continuums of structural polymorphs from each assembly population. This
25 discovery was revealed through the analysis of hundreds of individual fibrils in the population,

1 with the fibril structures subsequently hierarchically classified into polymorphic classes [25].
2 In this study, each individual fibril observed on AFM images was used to generate a 3D model
3 (e.g., left column in **Fig. 4c**), with no two fibril models being exactly the same. It is possible
4 that the morphological differences observed between closely related but not identical fibrils are
5 due to small variations in the helical twist and/or the packing of protofilaments with otherwise
6 identical core conformations, but the differences can also reflect structural variations of the
7 protofilament core, as illustrated in **Fig. 1**. Thus, the data demonstrates the potential of amyloid
8 fibrils to display strong structural individuality within the heterogeneous amyloid populations.
9
10 To date, AFM imaging has been used to characterise individual β -lactoglobulin amyloid fibrils
11 by measuring their height profile and twist pattern [49], as well as to analyse and compare the
12 morphologies of fibrils formed from wild-type α -synuclein and its disease-relevant variants
13 [50]. AFM has also been used to structurally characterise individual $A\beta_{40}$ filaments, which
14 revealed structurally polymorphic fibrils after long incubation times [46]. In addition, AFM
15 methods have helped to reveal that when samples containing different structural polymorphs,
16 identified by ssNMR, were used to seed new fibril samples, the elongation rate within the new
17 samples was specific to the structural polymorph of the seed [51], highlighting the relationship
18 between fibril structures and physicochemical properties such as kinetics. Furthermore,
19 developments in high-speed AFM have revealed the dynamics of individual $A\beta_{42}$ fibril
20 structures, including that elongation occurs preferentially at one end of the fibrils [52]. This is
21 a result that may contain clues to the organisation of protofilaments within individual fibrils.
22 AFM can also provide complementary structural information in combination with other
23 methods. An example of this includes the use of both AFM and cryo-EM to quantify the
24 structural variation in samples of diabetes-related IAPP fibrils, from which structures of the
25 fibril cores were also determined [53], or the use of ssNMR, cryo-EM and AFM to determine

1 the core structure of transthyretin fibrils [54]. Another example includes the use of AFM in
2 combination with fluorescence microscopy, in which evidence of structural variation within
3 individual fibrils was observed by AFM when mouse and hamster variant prion protein fibrils
4 were used to seed each other, resulting in individual fibrils with a conformational change [55].
5 Structural variations within individual fibrils have recently also been observed in *ex vivo*
6 samples of immunoglobulin light chain fibrils from patients with systemic AL amyloidosis and
7 in A β fibrils from patients with Alzheimer's disease (AD), both demonstrated using cryo-EM
8 [56,57]. Using AFM, we have observed strong individuality and structural variations within
9 A β_{1-42} fibrils formed *in vitro* (**Fig. 4**, middle column), demonstrating the extensive polymorphism
10 exhibited by A β sequences. Interestingly, AFM images of amyloid fibrils formed from tau₂₉₇₋₃₉₁
11 (also termed dGAE), with a morphology that mimics the core of paired helical filaments
12 extracted from Alzheimer's patient tissue [58], show little structural variations between
13 individual fibrils within its fibril population (**Fig. 4**, right column), suggesting that the extent
14 of structural polymorphism and fibril individuality is not the same for different amyloid
15 forming sequences.

16

17

18 **Physicochemical consequences of amyloid polymorphism**

19

20 Structural variations within and between individual fibrils in typically heterogeneous amyloid
21 populations can exist on multiple length scales (**Fig. 1**). These structural variations that define
22 amyloid polymorphism can range from atomic scale differences in the order of ångströms,
23 arising from packing variations of the polypeptide chains, to nanometre-scale variations in
24 fibril width, or even reach the scale of hundreds of nanometres in variations of twist periodicity
25 and handedness of amyloid fibrils [25]. At these different length scales, as a consequence of

1 the diversity and individuality of polymorphic amyloid structures, the physicochemical
2 properties of individual fibrils, such as the overall accessible surface area [45], surface
3 hydrophobicity and charge [59], growth and disassembly kinetics and thermodynamics [51],
4 and mechanical properties that include persistence length and the second moment of inertia
5 [60], can also vary within a population. Therefore, in contrast to globular proteins which
6 typically have a single native fold, the structural variation between individual fibrils within a
7 population may impact the functional properties of the amyloid population *in vivo*, mediated
8 by variation in their specific physicochemical properties. For example, different amyloid
9 structures have different cross-sectional dimensions and shapes. Thicker fibrils with rounded
10 cross-sections are likely to have a higher second moment of inertia than thin fibrils with
11 elliptical cross-sections, making them more resistant to breakage. Fibrils with higher
12 fragmentation rates are more likely to generate a larger number of small active amyloid
13 particles and subsequently may be more effective in propagating their amyloid state [61],
14 compared to fibrils that are more stable and less susceptible to breakage. This is demonstrated
15 through the size-dependent transfection efficiency relationship of Sup35NM amyloid particles
16 that confer the *[PSI⁻]* phenotype when transfected into yeast cells [62]. In studies of
17 transmissible amyloid known as prions, specific strains are found to selectively propagate from
18 cell to cell [63–66], suggesting a possible relationship between the strain phenomenon, the
19 structural polymorphism of amyloid fibrils, and the individual fibrils' stability towards
20 fragmentation. Thus, the differences in the stability of individual fibrils, as a consequence of
21 structural polymorphism, may lead to variations in the fitness of individual fibrils in an amyloid
22 population, and subsequent 'selection' of specific amyloid conformation due to a polymorphic
23 bias under certain conditions as well as adaptive 'evolution' processes of the dominant amyloid
24 conformation due to changes in the environment. The structural constraints provided by the
25 cross- β architecture coupled with a strong structural individuality in some amyloid populations,

1 and the ability of some amyloid to efficiently propagate the information encoded in their
2 conformational state, may suggest that some amyloid could behave in a manner similar to that
3 of viral quasispecies. In addition to fibril fragmentation, secondary nucleation is another
4 property that is affected by the fibril structural arrangement and could mediate the biological
5 effects of amyloid. Fibrils with a higher surface-area-to-volume ratio might provide better
6 access to active fibril surfaces that can catalyse secondary nucleation, compared to larger
7 amyloid structures with proportionally less available surface area. Secondary nucleation is a
8 process in which new amyloid are formed through catalysis by existing amyloid fibril surfaces.
9 The importance of secondary nucleation, in particular with respect to the biological impact of
10 $A\beta_{42}$ amyloid fibrils, has become increasingly evident. For example, by combining kinetic
11 analysis of $A\beta_{42}$ aggregation with impaired secondary nucleation using the molecular chaperone
12 Brichos [67] and antibodies that bind to the fibril surface [68], it has been shown that secondary
13 nucleation events may be the source of cytotoxic oligomeric species during $A\beta_{42}$ aggregation.
14 It is further possible, that secondary nucleation on the surface of amyloid fibrils is site-specific,
15 potentially occurring at sites of defects or at locations where structural breaks occur. Individual
16 fibril polymorphs with higher propensity to contain defects, have structural breaks, or those
17 that simply have a larger accessible surface area might then provide more efficient surfaces for
18 secondary nucleation, and, therefore, be responsible for a greater cytotoxic potential within the
19 amyloid population.

20

21 The polymorphic features of individual amyloid fibrils can both influence and be influenced
22 by interactions with other biological structures. For example, the formation of α -synuclein
23 amyloid fibrils *in vitro* is modulated by the air water interface [69]. Since α -synuclein fibrils
24 are found *in vivo* in patients with various diseases, where the air-water interface is likely to be
25 absent, it suggests that other biological interfaces may provide sites for the heterogeneous

1 nucleation of α -synuclein assembly. This type of surface-catalysed aggregation of
2 amyloidogenic proteins involves adsorption of amyloid forming proteins onto surfaces,
3 followed by a step that includes a conformational change, whether that be from a random coil
4 to the core fold of the resultant amyloid fibril or to an oligomeric intermediate state [70].
5 Importantly, the precise amyloid structures that form, amongst the diverse possible structures
6 that can be formed, may be dependent on the physicochemical characteristics of the catalysing
7 surface. High local concentrations of self-assembling proteins adsorbed onto a surface can
8 increase the rate of heterogeneous primary nucleation in a manner which is dependent on the
9 mobility of the proteins once adsorbed onto the surface. Cell membranes and, in particular,
10 their lipid bilayer components are amongst the most well-studied biological structures known
11 to interact with amyloidogenic proteins in such a manner [71–75]. Fibril formation reactions
12 can be catalysed by lipid bilayers [76,77], but can also be damaging to lipid bilayers [71,78,79].
13 In fact, it may be possible to connect the aggregation kinetics to the toxicity of the aggregation
14 reaction through their interaction with membranes [80]. In order for lipid bilayers to catalyse
15 primary nucleation, the monomeric subunits must first adsorb to the bilayer surface. In some
16 cases, lipid bilayers induce a conformational change in the monomeric subunits of an
17 amyloidogenic protein. For example, α -synuclein undergoes a change in conformation,
18 dependent on the fluidity of the lipid bilayer [81]. Additionally IAPP undergoes
19 conformational changes upon insertion into a lipid bilayer, eventually forming amyloid fibrils
20 in a lipid-mediated manner [82], and when mixed with large unilamellar vesicles it has been
21 observed that the secondary nucleation of $A\beta_{25}$ can be accelerated through lipid bilayer
22 interactions [76]. Conformational changes upon binding to a surface imply that structural
23 features of a resultant amyloid fibril can be dependent on the local physicochemical
24 environment, and the precise structures of the fibrils, therefore, will vary and contribute to the
25 individuality of each fibril in the population. Further biological structures which can impact

1 fibril formation include additional cell membrane constituents such as gangliosides [83],
2 extracellular structures such as heparin [84], as well as other heterologous amyloid fibrils
3 through cross-seeding events. If cross-seeding events proceed through surface-catalysed
4 reactions [42], the resulting new amyloid structures could result in considerable fibril diversity
5 and individuality, as heterogeneous nucleation events may also introduce heterogeneity in the
6 resulting amyloid population, depending on the physicochemical conditions of local interfaces.
7 Thus, surface interactions may enhance the potential for amyloid forming polypeptide
8 sequences to display structural polymorphism.

9

10

11 **Biological and pathological consequences of amyloid**

12 **polymorphism**

13

14 Amyloid fibrils display remarkable diversity in both the structures they form, as well as the
15 biological contexts they are found in. Some amyloid structures are found to be disease-
16 associated, while others may be essential for physiological functions. The wide range of *in vivo*
17 biological functions or pathological consequences of amyloid may reflect the polymorphic
18 diversity of amyloid fibril structures, mediated by the differing physicochemical properties of
19 individual amyloid fibrils, as discussed above. However, specific molecular links between
20 structural features, particular cellular pathways or processes, and biological consequences are
21 not currently well-understood. One of such possible mediating properties could be the
22 thermodynamic stability of the fibril core, determined by structural features like core
23 hydrophobicity and steric zipper interactions, with lower stability leading to reversible
24 assemblies [85,86]. Furthermore, amyloid with assembly-dependent functional roles may show
25 less polymorphism compared to disease-associated amyloid [85,87,88], which could indicate

1 that the specific core fold of amyloid fibrils may convey corresponding specific biological
2 properties that facilitate functional roles. In contrast, a wide range of polymorphs of disease-
3 associated amyloid structures have been observed, with diverse patterns of polymorphic extent
4 that include patient-specific polymorphism, clinical-subtype specific polymorphism for the
5 same disease, and disease-specific polymorphism (**Fig. 6**). Structural data obtained to date
6 suggest that different amyloid systems behave differently in this respect, although more
7 structural data of *ex vivo* amyloid assemblies is needed to resolve how the polymorphic
8 landscape varies in different disease-states, spatial localisations within organs, or individual
9 patients. Further structural characterisation of physiologically functional amyloid structures
10 and comparison of these structures with those of disease-associated amyloid is also necessary
11 to fundamentally understand the amyloid structure-function links.

12

13 Different neurodegenerative diseases show distinct patterns of spatial origins of amyloid
14 aggregation as well as progression by prion-like spreading, which is mediated by neuronal
15 connectivity and individual cell-type vulnerability [89]. For example, tau lesions originate in
16 different regions of the brain in patients with Alzheimer's disease and chronic traumatic
17 encephalopathy (CTE), despite being composed of the same protein isoforms [90]. The
18 structural diversity of the amyloid aggregates involved can be affected by the local *in vivo*
19 environment which could, in turn, elicit different biological effects based on the precise
20 physicochemical properties of the individual fibrils formed. These complex relationships may
21 result in biological feedback loops that subsequently contribute to the molecular and
22 phenotypical differences between amyloid-associated diseases, even when the primary
23 sequence of the original protein involved is identical. For example, in recent years, *ex vivo*
24 amyloid fibrils of the tau protein have been well-characterised, and their structures have been
25 resolved to high-resolution detail from the brain tissue of patients with various different

1 diseases, including Alzheimer's disease, Pick's disease, corticobasal degeneration (CBD) and
2 chronic traumatic encephalopathy [13–15,91]. Although tau isoforms forming the amyloid
3 fibrils differ between some diseases, and thus have slightly different primary sequences, the
4 structures of fibrils from Alzheimer's and CTE disease tissues, which both contain the 3R and
5 4R isoforms, are nevertheless different (**Fig. 6b**). Notably there is also polymorphism present
6 within the fibril population of each disease-specific sample, e.g., paired helical filaments (see
7 **Fig. 2** and **Table 2** entries 99, 108, 112 and 113) and straight filaments (see **Fig. 2** and **Table**
8 **2** entries 109, 114 and 115) in Alzheimer's disease brain tissue [13,92]. Other rare but
9 potentially also biologically important polymorphs of amyloid in the same disease-associated
10 amyloid populations may also be present [56], but their 3D structures are currently inaccessible
11 to characterisation by cryo-EM because they are present in low numbers, and therefore cannot
12 satisfy the extensive particle-averaging required by cryo-EM methodologies.

13

14 In addition to disease-specific amyloid polymorphism, considerable structural variation may
15 exist for A β amyloid from patients with different Alzheimer's disease clinical subtypes. Fibril
16 samples formed through seeding with *ex vivo* fibrils extracted from the brain cortex of patients
17 with Alzheimer's disease have been investigated by ssNMR [93]. While the structures of fibrils
18 formed from seeding do not necessarily reflect that of the seeds [40], it has been found that
19 seed samples originating from patients with prolonged-duration AD resulted in fibrils of a
20 single predominant A β_{40} polymorph, whereas samples originating from patients with rapidly
21 progressive AD resulted in a wider degree of structural diversity, suggesting that the seeds'
22 structures were different. A β amyloid fibrils from patient brain tissue with slowly and rapidly
23 progressing AD have also been shown to have different biochemical characteristics, including
24 different stability upon chemical and thermal denaturation, and higher levels of oligomeric A β_{42} .

1 in the rapidly progressive form [94], further evidencing the possible presence of complex,
2 clinical subtype-dependent amyloid polymorphism.

3
4 Cryo-EM structures from four patients with Alzheimer's disease have demonstrated common
5 paired helical and straight filament structures of tau amyloid [92], demonstrating that for some
6 amyloid assemblies, the structures are specific to the disease, and not to the individual patients
7 or disease subtypes. In addition, images of immunogold labelled tau amyloid fibril samples
8 from 19 AD patients, as well as from different brain regions of the same patients, also show
9 similar patterns. Subsequently, disease-specific fibril structures have been reported for various
10 tauopathies, giving rise to a structure-based classification approach for these neurodegenerative
11 diseases [12]. However, it is not yet known whether structures prevalent during earlier stages,
12 which may drive disease progression, are also identical to those extracted from the tissues of
13 individuals with end-stage AD and determined by cryo-EM.

14
15 Light chain (AL) amyloidosis is an example of patient-specific amyloid polymorphism. In AL
16 amyloidosis, expansion of a B cell clone leads to overproduction of a free monoclonal
17 immunoglobulin light chain protein, aggregation of which results in amyloid fibrils that
18 accumulate in organs, such as the heart or the kidneys, leading to tissue damage. The specific
19 sequence of the accumulating immunoglobulin light chain protein in each patient can affect the
20 propensity of amyloid formation and thus, potentially also the disease aetiology through impact
21 on the thermodynamic stability of the specific polypeptide sequence [95], the tissues where
22 amyloid deposits, and the clinical outcome [96]. However, it has been recently shown that
23 extrinsic factors, especially susceptibility to proteolytic cleavage and presence of proteases that
24 fragment the immunoglobulin light chain proteins under physiological conditions, could
25 instead be a strong determinant of amyloid formation *in vivo* [97]. Amyloid structures have

1 been resolved from the explanted cardiac tissue of three patients, demonstrating patient-
2 specific structural differences in detail [57,98,99]. Contrary to the previous examples of tau
3 and A β amyloid, the primary sequence of the monoclonal immunoglobulin light chain protein
4 varies between patients as it depends on the selection of the germline gene and somatic
5 mutations [100]. Thus, patient-specific amyloid polymorphism stems from the ‘top-level’
6 patient-specific variations in the primary polypeptide sequence (**Fig. 1** top row). It is, however,
7 not yet known whether patient-specific amyloid polymorphism can arise for amyloid structures
8 formed from the same monomeric polypeptide sequence. There remain currently many
9 unanswered questions on the *in vivo* role of amyloid in disease-states, both related to how the
10 environmental factors affect fibril growth and their structures, as well as how amyloid
11 formation and structures affect the surrounding cells and tissue environments, including any
12 cell-type specific vulnerabilities. Further insights into the relationship between fibril
13 polymorphism and their biological consequences can be achieved from continued efforts in
14 resolving *ex vivo* fibril structures from tissues of patients with different diagnoses or disease
15 progression, from different regions of the brain or diseased tissues, and from multiple
16 individual patients with the same diagnosis. Likewise, *in vitro* approaches in which the
17 polymorphic landscape is modified in a controlled manner by systematically varying sequence
18 or environmental factors to form specific structures will provide molecular and mechanistic
19 evidence of pathological pathways. Both approaches will equally require the structural
20 characterisation of amyloid fibrils to molecular and individual detail.

21

22

23 **Challenges in predicting the polymorphic landscape of amyloid** 24 **assembly**

25

1 For globular proteins, AlphaFold 2 did exceptionally well in predicting 3D structures from
2 primary amino-acid sequences [21]. The achievements of 3D structure prediction through deep
3 learning methods, e.g., the trained neural network architecture of AlphaFold 2, to date on
4 monomeric proteins in CASP14, is a result of both extensive computational resources for
5 model training and inference of new structures, as well as the availability of approximately
6 170,000 publicly available protein structure entries in the RCSB Protein Data Bank, and many
7 more protein sequences used for multiple sequence alignments, which inform structure
8 prediction. Future developments to AlphaFold 2 will potentially include prediction of protein
9 complexes. Although amyloid structures were not included as targets in CASP14, further
10 developments in structure prediction of large protein complexes, including amyloid, could lead
11 to fundamental understandings of how some of the biggest biological protein structures form.
12 Considerable developments to the current prediction methods will, however, need to be
13 incorporated to allow the prediction of many structures from a single primary sequence due to
14 the extensive polymorphism displayed by amyloid fibrils, which form diverse structures even
15 under identical environmental conditions and from identical amino acid sequences. This type
16 of challenge can only be met if a sufficiently holistic understanding of the assembly landscape,
17 in terms of both structures and energetics, is reached. However, with only around a hundred
18 amyloid fibril structures currently available in the PDB for full-length or fragments of
19 amyloidogenic proteins (**Table 2, Fig. 2**, not including cases where the same data has been
20 reanalysed), the limited training data available for structural prediction tool development,
21 especially ones that rely on ‘big-data’ approaches, pose a severe limitation to such a holistic
22 undertaking. A further 108 PDB structures are available for amyloid fibrils formed from
23 microcrystals of amyloid forming peptide sequences ranging from 4 to 11 amino acids in length,
24 determined by X-ray and electron diffraction techniques, which could be useful for the
25 prediction of local structural arrangements of the various steric-zipper motifs. Nevertheless, to

1 predict the structures of large, multi-polypeptide chain, and highly polymorphic protein
2 assemblies like amyloid, significant effort must first be spent on matching the quantity of high-
3 quality structural data, such as currently seen for globular proteins.

4

5 Another key challenge for amyloid structure prediction is the high potential sensitivity of the
6 amyloid conformation to a multitude of environmental factors, such as pH, ionic strength and
7 interactions with other biomolecules and surfaces. As the precise local *in vivo* environments
8 experienced by the various amyloid forming systems are unknown for disease-associated and
9 functional amyloid, the characterisation of *ex vivo* amyloid fibrils needs to be carried out as
10 indirect reporters on the relevant *in vivo* environments. These *in vivo* conditions are likely to
11 differ from conditions used *in vitro*, since *ex vivo* amyloid structures have been found to differ
12 compared to *in vitro* formed amyloid originating from monomers of the same amino acid
13 sequence [13,39,101]. Direct structural characterisation for *ex vivo* amyloid without the need
14 for further seeded amplification is currently only possible using cryo-EM. There are further
15 challenges for resolving *ex vivo* amyloid structures, including limited access to patient-derived
16 tissues, experimental challenges with extracting fibrils from these tissues, and the ability to
17 only study the most prevalent fibril species despite the diversity of species present. As a result,
18 currently, structural data of only fewer than thirty of such unseeded *ex vivo* amyloid have been
19 deposited to the EMDB and the PDB. Although an increasing number of *ex vivo* amyloid fibrils
20 are being studied every year, it remains a labour-intensive and costly endeavour. Thus, for
21 predicting the 3D structures of amyloid under physiologically relevant environmental
22 conditions, it may be necessary to first resolve how the assembly landscape is precisely
23 modulated by environmental conditions through combined *ex vivo* and *in vitro* approaches, and
24 then train a neural network using 3D structures formed under widely varying conditions.

25

1 The prediction of 3D protein structures gives rise to applications such as the ability to infer
2 function associated with the predicted structure, as well as structure-based drug design. These
3 applications rely on specific folds and motifs being predicted from amino acid sequences. For
4 amyloid, there are likely to be unique challenges compared to other, well-studied classes of
5 proteins such as enzymes, where a specific catalytic pocket could, for example, indicate a
6 specific functional role. As more structural data of amyloid from different biological contexts,
7 both disease-associated and functional, become available, it may be possible to predict whether
8 an amyloid forming sequence may be associated with the formation of assemblies with toxic
9 or infective potential. More structural data will facilitate this type of analysis and may
10 potentially reveal the mediating physicochemical factors involved in the link between amyloid
11 structure, function, and pathogenicity. Only once this relationship has been firmly established
12 based on both structural data and biological context, could a predicted 3D structure be used to
13 explore the potential biological consequences and aid structure-based therapeutic interventions.
14 A significant amyloid-specific opportunity for structure prediction lies in cases where
15 structures are disease subtype- or patient-specific. For example, in AL amyloidosis, each
16 patient has a slightly different immunoglobulin light chain amino acid sequence that can be
17 noninvasively determined from urine [102]. If the fibril structures could then be predicted from
18 the primary amino-acid sequence, it could be helpful in determining a specific clinical subtype
19 or indicate specific pathways of pathology. Furthermore, structure-based inhibitors of amyloid
20 aggregation have been demonstrated for some proteins such as A β in cell-culture models [103].
21 If a structure-based approach would be demonstrated to be clinically effective, for example,
22 for AL amyloidosis patients, prediction of structure from sequence could determine patient-
23 specific epitopes that could be targeted in a personalised medicine approach.

24

25

1 **Conclusions**

2

3 Amyloid assembly presents unique challenges to protein 3D structure elucidation, prediction,
4 and understanding of the relationship between structure and biological consequences.
5 Unresolved challenges arise from the highly polymorphic nature of amyloid assembly, the
6 subsequent individuality of each fibril formed within the heterogeneous amyloid populations,
7 and the resulting differences in the fibrils' physicochemical properties arising even from
8 monomers with identical amino acid sequences. This structural diversity is reflected in
9 amyloid-associated biological roles which range from functionality to pathogenic effects in
10 neurodegenerative diseases and systemic amyloidoses, with a potentially wide variation in
11 disease subtypes and clinical outcomes. Successful amyloid structure prediction from the
12 primary amino acid sequence of its monomeric polypeptide components will need to contain
13 robust predictions of whether an amino acid sequence is likely to form the cross- β amyloid
14 fold in the first place, followed by precise structural predictions that holistically takes into
15 account the assembly landscape and its sensitivity to the environmental conditions it
16 experiences. Finally, the path towards solving the 'one sequence to many structures' problem
17 amyloid assemblies represent, and the successful prediction of the full range of diverse amyloid
18 structures, will inevitably push our fundamental understanding of the coupled protein folding-
19 assembly processes commonly found in biology.

20

21

22 **Acknowledgements**

23

24 We thank Louise Serpell for all the discussions that inspired this review, as well as the members
25 of the Xue research group and the Kent Fungal Group for helpful comments throughout the

1 preparation of this manuscript. This work was supported by funding from the Biotechnology
2 and Biological Sciences Research Council (BBSRC), UK grant BB/S003312/1 (LDA and
3 WFX), as well as Engineering and Physical Sciences Research Council (EPSRC), UK DTP
4 grant EP/R513246/1 (LL).

5

6

7

1 **References**

2

- 3 [1] D. Eisenberg, M. Jucker, The amyloid state of proteins in human diseases, *Cell*. 148
4 (2012) 1188–1203. <https://doi.org/10.1016/j.cell.2012.02.022>.
- 5 [2] R. Riek, The three-dimensional structures of amyloids, *Cold Spring Harb. Perspect.*
6 *Biol.* 9 (2017) a023572. <https://doi.org/10.1101/cshperspect.a023572>.
- 7 [3] C.M. Dobson, T.P.J. Knowles, M. Vendruscolo, The amyloid phenomenon and its
8 significance in biology and medicine, *Cold Spring Harb. Perspect. Biol.* 12 (2020).
9 <https://doi.org/10.1101/cshperspect.a033878>.
- 10 [4] F. Chiti, C.M. Dobson, Protein misfolding, amyloid formation, and human disease: A
11 summary of progress over the last decade, *Annu. Rev. Biochem.* 86 (2017) 27–68.
12 <https://doi.org/10.1146/annurev-biochem-061516-045115>.
- 13 [5] M.D. Benson, J.N. Buxbaum, D.S. Eisenberg, G. Merlini, M.J.M. Saraiva, Y. Sekijima,
14 J.D. Sipe, P. Westermark, Amyloid nomenclature 2020: update and recommendations
15 by the International Society of Amyloidosis (ISA) nomenclature committee, *Amyloid*
16 *Int. J. Exp. Clin. Investig. Off. J. Int. Soc. Amyloidosis.* 27 (2020) 217–222.
17 <https://doi.org/10.1080/13506129.2020.1835263>.
- 18 [6] A.K. Buell, C.M. Dobson, T.P.J. Knowles, The physical chemistry of the amyloid
19 phenomenon: thermodynamics and kinetics of filamentous protein aggregation,
20 *Essays Biochem.* 56 (2014) 11–39. <https://doi.org/10.1042/bse0560011>.
- 21 [7] T.C.T. Michaels, A. Šarić, J. Habchi, S. Chia, G. Meisl, M. Vendruscolo, C.M. Dobson,
22 T.P.J. Knowles, Chemical kinetics for bridging molecular mechanisms and macroscopic
23 measurements of amyloid fibril formation, *Annu. Rev. Phys. Chem.* 69 (2018) 273–
24 298. <https://doi.org/10.1146/annurev-physchem-050317-021322>.

- 1 [8] W.-F. Xue, S.W. Homans, S.E. Radford, Systematic analysis of nucleation-dependent
2 polymerization reveals new insights into the mechanism of amyloid self-assembly,
3 Proc. Natl. Acad. Sci. 105 (2008) 8926–8931.
4 <https://doi.org/10.1073/pnas.0711664105>.
- 5 [9] S.I.A. Cohen, S. Linse, L.M. Luheshi, E. Hellstrand, D.A. White, L. Rajah, D.E. Otzen, M.
6 Vendruscolo, C.M. Dobson, T.P.J. Knowles, Proliferation of amyloid- β 42 aggregates
7 occurs through a secondary nucleation mechanism, Proc. Natl. Acad. Sci. 110 (2013)
8 9758–9763. <https://doi.org/10.1073/pnas.1218402110>.
- 9 [10] W.-F. Xue, A.L. Hellewell, W.S. Gosal, S.W. Homans, E.W. Hewitt, S.E. Radford, Fibril
10 fragmentation enhances amyloid cytotoxicity, J. Biol. Chem. 284 (2009) 34272–34282.
11 <https://doi.org/10.1074/jbc.M109.049809>.
- 12 [11] C. Scheckel, A. Aguzzi, Prions, prionoids and protein misfolding disorders, Nat. Rev.
13 Genet. 19 (2018) 405–418. <https://doi.org/10.1038/s41576-018-0011-4>.
- 14 [12] Y. Shi, W. Zhang, Y. Yang, A. Murzin, B. Falcon, A. Kotecha, M. van Beers, A. Tarutani,
15 F. Kametani, H.J. Garringer, R. Vidal, G.I. Hallinan, T. Lashley, Y. Saito, S. Murayama,
16 M. Yoshida, H. Tanaka, A. Kakita, T. Ikeuchi, A.C. Robinson, D.M.A. Mann, G.G. Kovacs,
17 T. Revesz, B. Ghetti, M. Hasegawa, M. Goedert, S.H.W. Scheres, Structure-based
18 classification of tauopathies, BioRxiv. (2021) 2021.05.28.446130.
19 <https://doi.org/10.1101/2021.05.28.446130>.
- 20 [13] A.W.P. Fitzpatrick, B. Falcon, S. He, A.G. Murzin, G. Murshudov, H.J. Garringer, R.A.
21 Crowther, B. Ghetti, M. Goedert, S.H.W. Scheres, Cryo-EM structures of tau filaments
22 from Alzheimer’s disease, Nature. 547 (2017) 185–190.
23 <https://doi.org/10.1038/nature23002>.

- 1 [14] W. Zhang, A. Tarutani, K.L. Newell, A.G. Murzin, T. Matsubara, B. Falcon, R. Vidal, H.J.
2 Garringer, Y. Shi, T. Ikeuchi, S. Murayama, B. Ghetti, M. Hasegawa, M. Goedert,
3 S.H.W. Scheres, Novel tau filament fold in corticobasal degeneration, *Nature*. 580
4 (2020) 283–287. <https://doi.org/10.1038/s41586-020-2043-0>.
- 5 [15] B. Falcon, J. Zivanov, W. Zhang, A.G. Murzin, H.J. Garringer, R. Vidal, R.A. Crowther,
6 K.L. Newell, B. Ghetti, M. Goedert, S.H.W. Scheres, Novel tau filament fold in chronic
7 traumatic encephalopathy encloses hydrophobic molecules, *Nature*. 568 (2019) 420–
8 423. <https://doi.org/10.1038/s41586-019-1026-5>.
- 9 [16] A.W. Fitzpatrick, H.R. Saibil, Cryo-EM of amyloid fibrils and cellular aggregates, *Curr.*
10 *Opin. Struct. Biol.* 58 (2019) 34–42. <https://doi.org/10.1016/j.sbi.2019.05.003>.
- 11 [17] R. Tycko, Solid state NMR studies of amyloid fibril structure, *Annu. Rev. Phys. Chem.*
12 62 (2011) 279–299. <https://doi.org/10.1146/annurev-physchem-032210-103539>.
- 13 [18] L. Lutter, C.J. Serpell, M.F. Tuite, L.C. Serpell, W.-F. Xue, Three-dimensional
14 reconstruction of individual helical nano-filament structures from atomic force
15 microscopy topographs, *Biomol. Concepts*. 11 (2020) 102–115.
16 <https://doi.org/10.1515/bmc-2020-0009>.
- 17 [19] F.S. Ruggeri, G. Longo, S. Faggiano, E. Lipiec, A. Pastore, G. Dietler, Infrared
18 nanospectroscopy characterization of oligomeric and fibrillar aggregates during
19 amyloid formation, *Nat. Commun.* 6 (2015) 7831.
20 <https://doi.org/10.1038/ncomms8831>.
- 21 [20] A.V. Krasnoslobodtsev, T. Deckert-Gaudig, Y. Zhang, V. Deckert, Y.L. Lyubchenko,
22 Polymorphism of amyloid fibrils formed by a peptide from the yeast prion protein
23 Sup35: AFM and Tip-Enhanced Raman Scattering studies, *Ultramicroscopy*. 165 (2016)
24 26–33. <https://doi.org/10.1016/j.ultramic.2016.03.011>.

- 1 [21] J. Jumper, R. Evans, A. Pritzel, T. Green, M. Figurnov, K. Tunyasuvunakool, O.
2 Ronneberger, R. Bates, A. Žídek, A. Bridgland, C. Meyer, S. Kohl, A. Potapenko, A.
3 Ballard, A. Cowie, B. Romera-Paredes, S. Mikolov, R. Jain, J. Adler, T. Back, S. Petersen,
4 D. Reiman, M. Steinegger, M. Pacholska, D. Silver, O. Vinyals, A. Senior, K.
5 Kavukcuoglu, P. Kohli, D. Hassabis, High accuracy protein structure prediction using
6 deep learning, (2020).
7 https://predictioncenter.org/casp14/doc/CASP14_Abstracts.pdf.
- 8 [22] A. Kryshtafovych, T. Schwede, M. Topf, K. Fidelis, J. Moult, Critical assessment of
9 methods of protein structure prediction (CASP)—Round XIII, *Proteins Struct. Funct.*
10 *Bioinforma.* 87 (2019) 1011–1020. <https://doi.org/10.1002/prot.25823>.
- 11 [23] J. Moult, K. Fidelis, A. Kryshtafovych, T. Schwede, A. Tramontano, Critical assessment
12 of methods of protein structure prediction (CASP)-Round XII, *Proteins.* 86 Suppl 1
13 (2018) 7–15. <https://doi.org/10.1002/prot.25415>.
- 14 [24] C.B. Anfinsen, Principles that govern the folding of protein chains, *Science.* 181 (1973)
15 223–230. <https://doi.org/10.1126/science.181.4096.223>.
- 16 [25] L.D. Aubrey, B.J.F. Blakeman, L. Lutter, C.J. Serpell, M.F. Tuite, L.C. Serpell, W.-F. Xue,
17 Quantification of amyloid fibril polymorphism by nano-morphometry reveals the
18 individuality of filament assembly, *Commun. Chem.* 3 (2020) 1–10.
19 <https://doi.org/10.1038/s42004-020-00372-3>.
- 20 [26] D. Li, C. Liu, Hierarchical chemical determination of amyloid polymorphs in
21 neurodegenerative disease, *Nat. Chem. Biol.* 17 (2021) 237–245.
22 <https://doi.org/10.1038/s41589-020-00708-z>.
- 23 [27] L. Lutter, C.J. Serpell, M.F. Tuite, W.-F. Xue, The molecular lifecycle of amyloid –
24 Mechanism of assembly, mesoscopic organisation, polymorphism, suprastructures,

- 1 and biological consequences, *Biochim. Biophys. Acta BBA - Proteins Proteomics*. 1867
2 (2019) 140257. <https://doi.org/10.1016/j.bbapap.2019.07.010>.
- 3 [28] D. Guzenko, A. Lafita, B. Monastyrskyy, A. Kryshchak, J.M. Duarte, Assessment of
4 protein assembly prediction in CASP13, *Proteins Struct. Funct. Bioinforma.* 87 (2019)
5 1190–1199. <https://doi.org/10.1002/prot.25795>.
- 6 [29] A.-M. Fernandez-Escamilla, F. Rousseau, J. Schymkowitz, L. Serrano, Prediction of
7 sequence-dependent and mutational effects on the aggregation of peptides and
8 proteins, *Nat. Biotechnol.* 22 (2004) 1302–1306. <https://doi.org/10.1038/nbt1012>.
- 9 [30] S. Maurer-Stroh, M. Debulpaep, N. Kuemmerer, M.L. de la Paz, I.C. Martins, J.
10 Reumers, K.L. Morris, A. Copland, L. Serpell, L. Serrano, J.W.H. Schymkowitz, F.
11 Rousseau, Exploring the sequence determinants of amyloid structure using position-
12 specific scoring matrices, *Nat. Methods*. 7 (2010) 237–242.
13 <https://doi.org/10.1038/nmeth.1432>.
- 14 [31] I. Walsh, F. Seno, S.C.E. Tosatto, A. Trovato, PASTA 2.0: an improved server for protein
15 aggregation prediction, *Nucleic Acids Res.* 42 (2014) W301–W307.
16 <https://doi.org/10.1093/nar/gku399>.
- 17 [32] B.P. Roland, R. Kodali, R. Mishra, R. Wetzel, A serendipitous survey of prediction
18 algorithms for amyloidogenicity, *Biopolymers*. 100 (2013) 780–789.
19 <https://doi.org/10.1002/bip.22305>.
- 20 [33] J. Santos, J. Pujols, I. Pallarès, V. Iglesias, S. Ventura, Computational prediction of
21 protein aggregation: Advances in proteomics, conformation-specific algorithms and
22 biotechnological applications, *Comput. Struct. Biotechnol. J.* 18 (2020) 1403–1413.
23 <https://doi.org/10.1016/j.csbj.2020.05.026>.

- 1 [34] T.R. Jahn, O.S. Makin, K.L. Morris, K.E. Marshall, P. Tian, P. Sikorski, L.C. Serpell, The
2 common architecture of cross- β amyloid, *J. Mol. Biol.* 395 (2010) 717–727.
3 <https://doi.org/10.1016/j.jmb.2009.09.039>.
- 4 [35] M.R. Sawaya, S. Sambashivan, R. Nelson, M.I. Ivanova, S.A. Sievers, M.I. Apostol, M.J.
5 Thompson, M. Balbirnie, J.J.W. Wiltzius, H.T. McFarlane, A.Ø. Madsen, C. Riek, D.
6 Eisenberg, Atomic structures of amyloid cross- β spines reveal varied steric zippers,
7 *Nature*. 447 (2007) 453–457. <https://doi.org/10.1038/nature05695>.
- 8 [36] J.A. Rodriguez, M.I. Ivanova, M.R. Sawaya, D. Cascio, F.E. Reyes, D. Shi, S. Sangwan,
9 E.L. Guenther, L.M. Johnson, M. Zhang, L. Jiang, M.A. Arbing, B.L. Nannenga, J. Hattne,
10 J. Whitelegge, A.S. Brewster, M. Messerschmidt, S. Boutet, N.K. Sauter, T. Gonen, D.S.
11 Eisenberg, Structure of the toxic core of α -synuclein from invisible crystals, *Nature*.
12 525 (2015) 486–490. <https://doi.org/10.1038/nature15368>.
- 13 [37] S.H.W. Scheres, Amyloid structure determination in RELION-3.1, *Acta Crystallogr.*
14 *Sect. Struct. Biol.* 76 (2020) 94–101. <https://doi.org/10.1107/S2059798319016577>.
- 15 [38] T. Arakhamia, C.E. Lee, Y. Carlomagno, D.M. Duong, S.R. Kundinger, K. Wang, D.
16 Williams, M. DeTure, D.W. Dickson, C.N. Cook, N.T. Seyfried, L. Petrucelli, A.W.P.
17 Fitzpatrick, Posttranslational modifications mediate the structural diversity of
18 tauopathy strains, *Cell*. 180 (2020) 633–644.e12.
19 <https://doi.org/10.1016/j.cell.2020.01.027>.
- 20 [39] A. Bansal, M. Schmidt, M. Rennegarbe, C. Haupt, F. Liberta, S. Stecher, I. Puscalau-
21 Girtu, A. Biedermann, M. Fändrich, AA amyloid fibrils from diseased tissue are
22 structurally different from in vitro formed SAA fibrils, *Nat. Commun.* 12 (2021) 1013.
23 <https://doi.org/10.1038/s41467-021-21129-z>.

- 1 [40] S. Lövestam, M. Schweighauser, T. Matsubara, S. Murayama, T. Tomita, T. Ando, K.
2 Hasegawa, M. Yoshida, A. Tarutani, M. Hasegawa, M. Goedert, S.H.W. Scheres,
3 Seeded assembly *in vitro* does not replicate the structures of α -synuclein filaments
4 from multiple system atrophy, FEBS Open Bio. (2021). [https://doi.org/10.1002/2211-](https://doi.org/10.1002/2211-5463.13110)
5 5463.13110.
- 6 [41] G. Meisl, X. Yang, E. Hellstrand, B. Frohm, J.B. Kirkegaard, S.I.A. Cohen, C.M. Dobson,
7 S. Linse, T.P.J. Knowles, Differences in nucleation behavior underlie the contrasting
8 aggregation kinetics of the A β 40 and A β 42 peptides, Proc. Natl. Acad. Sci. 111 (2014)
9 9384–9389. <https://doi.org/10.1073/pnas.1401564111>.
- 10 [42] N. Koloteva-Levine, R. Marchante, T.J. Purton, J.R. Hiscock, M.F. Tuite, W.-F. Xue,
11 Amyloid particles facilitate surface-catalyzed cross-seeding by acting as promiscuous
12 nanoparticles, BioRxiv. (2020) 2020.09.01.278481.
13 <https://doi.org/10.1101/2020.09.01.278481>.
- 14 [43] A. Peduzzo, S. Linse, A.K. Buell, The properties of α -synuclein secondary nuclei are
15 dominated by the solution conditions rather than the seed fibril strain, ACS Chem.
16 Neurosci. 11 (2020) 909–918. <https://doi.org/10.1021/acscchemneuro.9b00594>.
- 17 [44] J. Adamcik, R. Mezzenga, Study of amyloid fibrils via atomic force microscopy, Curr.
18 Opin. Colloid Interface Sci. 17 (2012) 369–376.
19 <https://doi.org/10.1016/j.cocis.2012.08.001>.
- 20 [45] M. Fändrich, J. Meinhardt, N. Grigorieff, Structural polymorphism of Alzheimer A β
21 and other amyloid fibrils, Prion. 3 (2009) 89–93. <https://doi.org/10.4161/pri.3.2.8859>.
- 22 [46] C. Goldsbury, P. Frey, V. Olivieri, U. Aebi, S.A. Müller, Multiple assembly pathways
23 underlie amyloid- β fibril polymorphisms, J. Mol. Biol. 352 (2005) 282–298.
24 <https://doi.org/10.1016/j.jmb.2005.07.029>.

- 1 [47] J.L. Jiménez, E.J. Nettleton, M. Bouchard, C.V. Robinson, C.M. Dobson, H.R. Saibil, The
2 protofilament structure of insulin amyloid fibrils, *Proc. Natl. Acad. Sci. U. S. A.* 99
3 (2002) 9196–9201. <https://doi.org/10.1073/pnas.142459399>.
- 4 [48] N.M. Kad, S.L. Myers, D.P. Smith, D. Alastair Smith, S.E. Radford, N.H. Thomson,
5 Hierarchical assembly of β 2-microglobulin amyloid *in vitro* revealed by atomic force
6 microscopy, *J. Mol. Biol.* 330 (2003) 785–797. [https://doi.org/10.1016/S0022-](https://doi.org/10.1016/S0022-2836(03)00583-7)
7 2836(03)00583-7.
- 8 [49] J. Adamcik, J.-M. Jung, J. Flakowski, P. De Los Rios, G. Dietler, R. Mezzenga,
9 Understanding amyloid aggregation by statistical analysis of atomic force microscopy
10 images, *Nat. Nanotechnol.* 5 (2010) 423–428.
11 <https://doi.org/10.1038/nnano.2010.59>.
- 12 [50] F.S. Ruggeri, P. Flagmeier, J.R. Kumita, G. Meisl, D.Y. Chirgadze, M.N. Bongiovanni,
13 T.P.J. Knowles, C.M. Dobson, The influence of pathogenic mutations in α -synuclein on
14 biophysical and structural characteristics of amyloid fibrils, *ACS Nano.* 14 (2020)
15 5213–5222. <https://doi.org/10.1021/acsnano.9b09676>.
- 16 [51] W. Qiang, K. Kelley, R. Tycko, Polymorph-specific kinetics and thermodynamics of β -
17 amyloid fibril growth, *J. Am. Chem. Soc.* 135 (2013) 6860–6871.
18 <https://doi.org/10.1021/ja311963f>.
- 19 [52] T. Watanabe-Nakayama, K. Ono, M. Itami, R. Takahashi, D.B. Teplow, M. Yamada,
20 High-speed atomic force microscopy reveals structural dynamics of amyloid β_{1-42}
21 aggregates, *Proc. Natl. Acad. Sci.* 113 (2016) 5835–5840.
22 <https://doi.org/10.1073/pnas.1524807113>.
- 23 [53] R. Gallardo, M.G. Iadanza, Y. Xu, G.R. Heath, R. Foster, S.E. Radford, N.A. Ranson,
24 Fibril structures of diabetes-related amylin variants reveal a basis for surface-

- 1 templated assembly, *Nat. Struct. Mol. Biol.* 27 (2020) 1048–1056.
2 <https://doi.org/10.1038/s41594-020-0496-3>.
- 3 [54] A.W.P. Fitzpatrick, G.T. Debelouchina, M.J. Bayro, D.K. Clare, M.A. Caporini, V.S. Bajaj,
4 C.P. Jaroniec, L. Wang, V. Ladizhansky, S.A. Müller, C.E. MacPhee, C.A. Waudby, H.R.
5 Mott, A.D. Simone, T.P.J. Knowles, H.R. Saibil, M. Vendruscolo, E.V. Orlova, R.G.
6 Griffin, C.M. Dobson, Atomic structure and hierarchical assembly of a cross- β amyloid
7 fibril, *Proc. Natl. Acad. Sci.* 110 (2013) 5468–5473.
8 <https://doi.org/10.1073/pnas.1219476110>.
- 9 [55] N. Makarava, V.G. Ostapchenko, R. Savtchenko, I.V. Baskakov, Conformational
10 switching within individual amyloid fibrils, *J. Biol. Chem.* 284 (2009) 14386–14395.
11 <https://doi.org/10.1074/jbc.M900533200>.
- 12 [56] M. Kollmer, W. Close, L. Funk, J. Rasmussen, A. Bsoul, A. Schierhorn, M. Schmidt, C.J.
13 Sigurdson, M. Jucker, M. Fändrich, Cryo-EM structure and polymorphism of A β
14 amyloid fibrils purified from Alzheimer’s brain tissue, *Nat. Commun.* 10 (2019).
15 <https://doi.org/10.1038/s41467-019-12683-8>.
- 16 [57] L. Rademaker, J. Baur, S. Huhn, C. Haupt, U. Hegenbart, S. Schönland, A. Bansal, M.
17 Schmidt, M. Fändrich, Cryo-EM reveals structural breaks in a patient-derived amyloid
18 fibril from systemic AL amyloidosis, *Nat. Commun.* 12 (2021) 875.
19 <https://doi.org/10.1038/s41467-021-21126-2>.
- 20 [58] Y.K. Al-Hilaly, B.E. Foster, L. Biasetti, L. Lutter, S.J. Pollack, J.E. Rickard, J.M.D. Storey,
21 C.R. Harrington, W.-F. Xue, C.M. Wischik, L.C. Serpell, Tau (297-391) forms filaments
22 that structurally mimic the core of paired helical filaments in Alzheimer’s disease
23 brain, *FEBS Lett.* 594 (2020) 944–950. <https://doi.org/10.1002/1873-3468.13675>.

- 1 [59] J. Pansieri, M.A. Halim, C. Vendrely, M. Dumoulin, F. Legrand, M.M. Sallanon, S.
2 Chierici, S. Denti, X. Dagany, P. Dugourd, C. Marquette, R. Antoine, V. Forge, Mass and
3 charge distributions of amyloid fibers involved in neurodegenerative diseases:
4 mapping heterogeneity and polymorphism, *Chem. Sci.* 9 (2018) 2791–2796.
5 <https://doi.org/10.1039/C7SC04542E>.
- 6 [60] T.P. Knowles, A.W. Fitzpatrick, S. Meehan, H.R. Mott, M. Vendruscolo, C.M. Dobson,
7 M.E. Welland, Role of intermolecular forces in defining material properties of protein
8 nanofibrils, *Science*. 318 (2007) 1900–1903.
9 <https://doi.org/10.1126/science.1150057>.
- 10 [61] D.M. Beal, M. Tournus, R. Marchante, T.J. Purton, D.P. Smith, M.F. Tuite, M. Doumic,
11 W.-F. Xue, The division of amyloid fibrils: Systematic comparison of fibril
12 fragmentation stability by linking theory with experiments, *IScience*. 23 (2020)
13 101512. <https://doi.org/10.1016/j.isci.2020.101512>.
- 14 [62] R. Marchante, D.M. Beal, N. Koloteva-Levine, T.J. Purton, M.F. Tuite, W.-F. Xue, The
15 physical dimensions of amyloid aggregates control their infective potential as prion
16 particles, *ELife*. 6 (2017) e27109. <https://doi.org/10.7554/eLife.27109>.
- 17 [63] R. Atarashi, V.L. Sim, N. Nishida, B. Caughey, S. Katamine, Prion strain-dependent
18 differences in conversion of mutant prion proteins in cell culture, *J. Virol.* 80 (2006)
19 7854–7862. <https://doi.org/10.1128/JVI.00424-06>.
- 20 [64] D.A. Bateman, R.B. Wickner, The $[PSI^+]$ prion exists as a dynamic cloud of variants,
21 *PLOS Genet.* 9 (2013) e1003257. <https://doi.org/10.1371/journal.pgen.1003257>.
- 22 [65] M.E. Bruce, I. McConnell, H. Fraser, A.G. Dickinson, The disease characteristics of
23 different strains of scrapie in *Sinc* congenic mouse lines: implications for the nature of

- 1 the agent and host control of pathogenesis, *J. Gen. Virol.* 72 (Pt 3) (1991) 595–603.
2 <https://doi.org/10.1099/0022-1317-72-3-595>.
- 3 [66] S. Hannaoui, L. Maatouk, N. Privat, E. Levavasseur, B.A. Faucheux, S. Haïk, Prion
4 propagation and toxicity occur *in vitro* with two-phase kinetics specific to strain and
5 neuronal type, *J. Virol.* 87 (2013) 2535–2548. <https://doi.org/10.1128/JVI.03082-12>.
- 6 [67] S.I.A. Cohen, P. Arosio, J. Presto, F.R. Kurudenkandy, H. Biverstål, L. Dolfe, C. Dunning,
7 X. Yang, B. Frohm, M. Vendruscolo, J. Johansson, C.M. Dobson, A. Fisahn, T.P.J.
8 Knowles, S. Linse, A molecular chaperone breaks the catalytic cycle that generates
9 toxic A β oligomers, *Nat. Struct. Mol. Biol.* 22 (2015) 207–213.
10 <https://doi.org/10.1038/nsmb.2971>.
- 11 [68] T.C.T. Michaels, A. Šarić, G. Meisl, G.T. Heller, S. Curk, P. Arosio, S. Linse, C.M. Dobson,
12 M. Vendruscolo, T.P.J. Knowles, Thermodynamic and kinetic design principles for
13 amyloid-aggregation inhibitors, *Proc. Natl. Acad. Sci.* 117 (2020) 24251–24257.
14 <https://doi.org/10.1073/pnas.2006684117>.
- 15 [69] S. Campioni, G. Carret, S. Jordens, L. Nicoud, R. Mezzenga, R. Riek, The presence of an
16 air–water interface affects formation and elongation of α -synuclein fibrils, *J. Am.*
17 *Chem. Soc.* 136 (2014) 2866–2875. <https://doi.org/10.1021/ja412105t>.
- 18 [70] F. Grigolato, P. Arosio, The role of surfaces on amyloid formation, *Biophys. Chem.* 270
19 (2021) 106533. <https://doi.org/10.1016/j.bpc.2020.106533>.
- 20 [71] D.C. Bode, M.D. Baker, J.H. Viles, Ion channel formation by amyloid- β_{42} oligomers but
21 not amyloid- β_{40} in cellular membranes, *J. Biol. Chem.* 292 (2017) 1404–1413.
22 <https://doi.org/10.1074/jbc.M116.762526>.

- 1 [72] S.M. Butterfield, H.A. Lashuel, Amyloidogenic protein–membrane interactions:
2 Mechanistic insight from model systems, *Angew. Chem. Int. Ed.* 49 (2010) 5628–5654.
3 <https://doi.org/10.1002/anie.200906670>.
- 4 [73] L. Milanesi, T. Sheynis, W.-F. Xue, E.V. Orlova, A.L. Hellewell, R. Jelinek, E.W. Hewitt,
5 S.E. Radford, H.R. Saibil, Direct three-dimensional visualization of membrane
6 disruption by amyloid fibrils, *Proc. Natl. Acad. Sci.* 109 (2012) 20455–20460.
7 <https://doi.org/10.1073/pnas.1206325109>.
- 8 [74] E. Monsellier, L. Bousset, R. Melki, α -Synuclein and huntingtin exon 1 amyloid fibrils
9 bind laterally to the cellular membrane, *Sci. Rep.* 6 (2016) 19180.
10 <https://doi.org/10.1038/srep19180>.
- 11 [75] M.F.M. Sciacca, C. Tempra, F. Scollo, D. Milardi, C. La Rosa, Amyloid growth and
12 membrane damage: Current themes and emerging perspectives from theory and
13 experiments on A β and hIAPP, *Biochim. Biophys. Acta BBA - Biomembr.* 1860 (2018)
14 1625–1638. <https://doi.org/10.1016/j.bbamem.2018.02.022>.
- 15 [76] D.J. Lindberg, E. Wesén, J. Björkeröth, S. Rocha, E.K. Esbjörner, Lipid membranes
16 catalyse the fibril formation of the amyloid- β (1-42) peptide through lipid-fibril
17 interactions that reinforce secondary pathways, *Biochim. Biophys. Acta Biomembr.*
18 1859 (2017) 1921–1929. <https://doi.org/10.1016/j.bbamem.2017.05.012>.
- 19 [77] A. Vahdat Shariat Panahi, P. Hultman, K. Öllinger, G.T. Westermark, K. Lundmark,
20 Lipid membranes accelerate amyloid formation in the mouse model of AA
21 amyloidosis, *Amyloid Int. J. Exp. Clin. Investig. Off. J. Int. Soc. Amyloidosis.* 26 (2019)
22 34–44. <https://doi.org/10.1080/13506129.2019.1576606>.
- 23 [78] E. Sparr, M.F.M. Engel, D.V. Sakharov, M. Sprong, J. Jacobs, B. de Kruijff, J.W.M.
24 Höppener, J.A. Killian, Islet amyloid polypeptide-induced membrane leakage involves

- 1 uptake of lipids by forming amyloid fibers, FEBS Lett. 577 (2004) 117–120.
2 <https://doi.org/10.1016/j.febslet.2004.09.075>.
- 3 [79] M.F.M. Engel, L. Khemtémourian, C.C. Kleijer, H.J.D. Meeldijk, J. Jacobs, A.J. Verkleij,
4 B. de Kruijff, J.A. Killian, J.W.M. Höppener, Membrane damage by human islet
5 amyloid polypeptide through fibril growth at the membrane, Proc. Natl. Acad. Sci. 105
6 (2008) 6033–6038. <https://doi.org/10.1073/pnas.0708354105>.
- 7 [80] P. Flagmeier, S. De, T.C.T. Michaels, X. Yang, A.J. Dear, C. Emanuelsson, M.
8 Vendruscolo, S. Linse, D. Klenerman, T.P.J. Knowles, C.M. Dobson, Direct
9 measurement of lipid membrane disruption connects kinetics and toxicity of A β 42
10 aggregation, Nat. Struct. Mol. Biol. 27 (2020) 886–891.
11 <https://doi.org/10.1038/s41594-020-0471-z>.
- 12 [81] M. Rovere, J.B. Sanderson, L. Fonseca-Ornelas, D.S. Patel, T. Bartels, Refolding of
13 helical soluble α -synuclein through transient interaction with lipid interfaces, FEBS
14 Lett. 592 (2018) 1464–1472. <https://doi.org/10.1002/1873-3468.13047>.
- 15 [82] K. Sasahara, K. Morigaki, T. Okazaki, D. Hamada, Binding of islet amyloid polypeptide
16 to supported lipid bilayers and amyloid aggregation at the membranes, Biochemistry.
17 51 (2012) 6908–6919. <https://doi.org/10.1021/bi300542g>.
- 18 [83] A. Kakio, S. Nishimoto, K. Yanagisawa, Y. Kozutsumi, K. Matsuzaki, Interactions of
19 amyloid β -protein with various gangliosides in raft-like membranes: Importance of
20 GM1 ganglioside-bound form as an endogenous seed for Alzheimer amyloid,
21 Biochemistry. 41 (2002) 7385–7390. <https://doi.org/10.1021/bi0255874>.
- 22 [84] M. Goedert, R. Jakes, M.G. Spillantini, M. Hasegawa, M.J. Smith, R.A. Crowther,
23 Assembly of microtubule-associated protein tau into Alzheimer-like filaments induced

- 1 by sulphated glycosaminoglycans, *Nature*. 383 (1996) 550–553.
- 2 <https://doi.org/10.1038/383550a0>.
- 3 [85] J. Lu, Q. Cao, M.P. Hughes, M.R. Sawaya, D.R. Boyer, D. Cascio, D.S. Eisenberg,
4 CryoEM structure of the low-complexity domain of hnRNPA2 and its conversion to
5 pathogenic amyloid, *Nat. Commun.* 11 (2020) 4090. [https://doi.org/10.1038/s41467-](https://doi.org/10.1038/s41467-020-17905-y)
6 [020-17905-y](https://doi.org/10.1038/s41467-020-17905-y).
- 7 [86] S.M. Ulamec, S.E. Radford, Spot the difference: Function versus toxicity in amyloid
8 fibrils, *Trends Biochem. Sci.* (2020). <https://doi.org/10.1016/j.tibs.2020.04.007>.
- 9 [87] R. Hervas, M.J. Rau, Y. Park, W. Zhang, A.G. Murzin, J.A.J. Fitzpatrick, S.H.W. Scheres,
10 K. Si, Cryo-EM structure of a neuronal functional amyloid implicated in memory
11 persistence in *Drosophila*, *Science*. 367 (2020) 1230–1234.
12 <https://doi.org/10.1126/science.aba3526>.
- 13 [88] D.T. Murray, M. Kato, Y. Lin, K.R. Thurber, I. Hung, S.L. McKnight, R. Tycko, Structure
14 of FUS protein fibrils and its relevance to self-assembly and phase separation of low-
15 complexity domains, *Cell*. 171 (2017) 615-627.e16.
16 <https://doi.org/10.1016/j.cell.2017.08.048>.
- 17 [89] J. Brettschneider, K.D. Tredici, V.M.-Y. Lee, J.Q. Trojanowski, Spreading of pathology in
18 neurodegenerative diseases: a focus on human studies, *Nat. Rev. Neurosci.* 16 (2015)
19 109–120. <https://doi.org/10.1038/nrn3887>.
- 20 [90] A. Katsumoto, H. Takeuchi, F. Tanaka, Tau pathology in chronic traumatic
21 encephalopathy and Alzheimer’s disease: Similarities and differences, *Front. Neurol.*
22 10 (2019). <https://doi.org/10.3389/fneur.2019.00980>.
- 23 [91] B. Falcon, W. Zhang, A.G. Murzin, G. Murshudov, H.J. Garringer, R. Vidal, R.A.
24 Crowther, B. Ghetti, S.H.W. Scheres, M. Goedert, Structures of filaments from Pick’s

- 1 disease reveal a novel tau protein fold, *Nature*. (2018) 1.
2 <https://doi.org/10.1038/s41586-018-0454-y>.
- 3 [92] B. Falcon, W. Zhang, M. Schweighauser, A.G. Murzin, R. Vidal, H.J. Garringer, B.
4 Ghetti, S.H.W. Scheres, M. Goedert, Tau filaments from multiple cases of sporadic and
5 inherited Alzheimer's disease adopt a common fold, *Acta Neuropathol. (Berl.)*. 136
6 (2018) 699–708. <https://doi.org/10.1007/s00401-018-1914-z>.
- 7 [93] W. Qiang, W.-M. Yau, J.-X. Lu, J. Collinge, R. Tycko, Structural variation in amyloid- β
8 fibrils from Alzheimer's disease clinical subtypes, *Nature*. 541 (2017) 217–221.
9 <https://doi.org/10.1038/nature20814>.
- 10 [94] M.L. Cohen, C. Kim, T. Haldiman, M. ElHag, P. Mehndiratta, T. Pichet, F. Lissemore, M.
11 Shea, Y. Cohen, W. Chen, J. Blevins, B.S. Appleby, K. Surewicz, W.K. Surewicz, M.
12 Sajatovic, C. Tatsuoka, S. Zhang, P. Mayo, M. Butkiewicz, J.L. Haines, A.J. Lerner, J.G.
13 Safar, Rapidly progressive Alzheimer's disease features distinct structures of amyloid-
14 β , *Brain J. Neurol.* 138 (2015) 1009–1022. <https://doi.org/10.1093/brain/awv006>.
- 15 [95] C.N. Nokwe, M. Hora, M. Zacharias, H. Yagi, J. Peschek, B. Reif, Y. Goto, J. Buchner, A
16 stable mutant predisposes antibody domains to amyloid formation through specific
17 non-native interactions, *J. Mol. Biol.* 428 (2016) 1315–1332.
18 <https://doi.org/10.1016/j.jmb.2016.01.015>.
- 19 [96] R.S. Abraham, S.M. Geyer, T.L. Price-Troska, C. Allmer, R.A. Kyle, M.A. Gertz, R.
20 Fonseca, Immunoglobulin light chain variable (V) region genes influence clinical
21 presentation and outcome in light chain-associated amyloidosis (AL), *Blood*. 101
22 (2003) 3801–3807. <https://doi.org/10.1182/blood-2002-09-2707>.
- 23 [97] R. Sterneke-Hoffmann, T. Pauly, R.K. Norrild, J. Hansen, M. Dupré, F. Tucholski, M.
24 Duchateau, M. Rey, S. Metzger, A. Boquoi, F. Platten, S.U. Egelhaaf, J. Chamot-Rooke,

- 1 R. Fenk, L. Nagel-Steger, R. Haas, A.K. Buell, Universal amyloidogenicity of patient-
2 derived immunoglobulin light chains, *BioRxiv*. (2021) 2021.05.12.443858.
3 <https://doi.org/10.1101/2021.05.12.443858>.
- 4 [98] L. Rademaker, Y.-H. Lin, K. Annamalai, S. Huhn, U. Hegenbart, S.O. Schönland, G. Fritz,
5 M. Schmidt, M. Fändrich, Cryo-EM structure of a light chain-derived amyloid fibril
6 from a patient with systemic AL amyloidosis, *Nat. Commun.* 10 (2019) 1103.
7 <https://doi.org/10.1038/s41467-019-09032-0>.
- 8 [99] P. Swuec, F. Lavatelli, M. Tasaki, C. Paisonni, P. Rognoni, M. Maritan, F. Brambilla, P.
9 Milani, P. Mauri, C. Camilloni, G. Palladini, G. Merlini, S. Ricagno, M. Bolognesi, Cryo-
10 EM structure of cardiac amyloid fibrils from an immunoglobulin light chain AL
11 amyloidosis patient, *Nat. Commun.* 10 (2019) 1269. [https://doi.org/10.1038/s41467-](https://doi.org/10.1038/s41467-019-09133-w)
12 [019-09133-w](https://doi.org/10.1038/s41467-019-09133-w).
- 13 [100] L.M. Blancas-Mejia, P. Misra, C.J. Dick, S.A. Cooper, K.R. Redhage, M.R. Bergman, T.L.
14 Jordan, K. Maar, M. Ramirez-Alvarado, Immunoglobulin light chain amyloid
15 aggregation, *Chem. Commun. Camb. Engl.* 54 (2018) 10664–10674.
16 <https://doi.org/10.1039/c8cc04396e>.
- 17 [101] W. Zhang, B. Falcon, A.G. Murzin, J. Fan, R.A. Crowther, M. Goedert, S.H. Scheres,
18 Heparin-induced tau filaments are polymorphic and differ from those in Alzheimer's
19 and Pick's diseases, *ELife.* 8 (2019) e43584. <https://doi.org/10.7554/eLife.43584>.
- 20 [102] A. Solomon, D.T. Weiss, C.L. Murphy, R. Hrnčić, J.S. Wall, M. Schell, Light chain-
21 associated amyloid deposits comprised of a novel κ constant domain, *Proc. Natl.*
22 *Acad. Sci.* 95 (1998) 9547–9551. <https://doi.org/10.1073/pnas.95.16.9547>.
- 23 [103] S.L. Griner, P. Seidler, J. Bowler, K.A. Murray, T.P. Yang, S. Sahay, M.R. Sawaya, D.
24 Cascio, J.A. Rodriguez, S. Philipp, J. Sosna, C.G. Glabe, T. Gonen, D.S. Eisenberg,

- 1 Structure-based inhibitors of amyloid beta core suggest a common interface with tau,
2 ELife. 8 (2019) e46924. <https://doi.org/10.7554/eLife.46924>.
- 3 [104] E.F. Pettersen, T.D. Goddard, C.C. Huang, G.S. Couch, D.M. Greenblatt, E.C. Meng, T.E.
4 Ferrin, UCSF Chimera--a visualization system for exploratory research and analysis, J.
5 Comput. Chem. 25 (2004) 1605–1612. <https://doi.org/10.1002/jcc.20084>.
- 6 [105] U. Ghosh, K.R. Thurber, W.-M. Yau, R. Tycko, Molecular structure of a prevalent
7 amyloid- β fibril polymorph from Alzheimer's disease brain tissue, Proc. Natl. Acad.
8 Sci. 118 (2021) e2023089118. <https://doi.org/10.1073/pnas.2023089118>.
- 9 [106] L. Cerofolini, E. Ravera, S. Bologna, T. Wiglenda, A. Böddrich, B. Purfürst, I. Benilova,
10 M. Korsak, G. Gallo, D. Rizzo, L. Gonnelli, M. Fragai, B.D. Strooper, E.E. Wanker, C.
11 Luchinat, Mixing A β (1–40) and A β (1–42) peptides generates unique amyloid fibrils,
12 Chem. Commun. 56 (2020) 8830–8833. <https://doi.org/10.1039/D0CC02463E>.
- 13 [107] Z.-W. Hu, L. Vugmeyster, D.F. Au, D. Ostrovsky, Y. Sun, W. Qiang, Molecular structure
14 of an N-terminal phosphorylated β -amyloid fibril, Proc. Natl. Acad. Sci. 116 (2019)
15 11253–11258. <https://doi.org/10.1073/pnas.1818530116>.
- 16 [108] A. Rohou, N. Grigorieff, Frealix: Model-based refinement of helical filament structures
17 from electron micrographs, J. Struct. Biol. 186 (2014) 234–244.
18 <https://doi.org/10.1016/j.jsb.2014.03.012>.
- 19 [109] N.G. Sgourakis, W.-M. Yau, W. Qiang, Modeling an in-register, parallel “Iowa” A β fibril
20 structure using solid-state NMR data from labeled samples with Rosetta, Structure. 23
21 (2015) 216–227. <https://doi.org/10.1016/j.str.2014.10.022>.
- 22 [110] A.K. Schütz, T. Vagt, M. Huber, O.Y. Ovchinnikova, R. Cadalbert, J. Wall, P. Güntert, A.
23 Böckmann, R. Glockshuber, B.H. Meier, Atomic-resolution three-dimensional

- 1 structure of amyloid β fibrils bearing the Osaka mutation, *Angew. Chem. Int. Ed.* 54
2 (2015) 331–335. <https://doi.org/10.1002/anie.201408598>.
- 3 [111] J.-X. Lu, W. Qiang, W.-M. Yau, C.D. Schwieters, S.C. Meredith, R. Tycko, *Molecular*
4 structure of β -amyloid fibrils in Alzheimer's disease brain tissue, *Cell*. 154 (2013)
5 1257–1268. <https://doi.org/10.1016/j.cell.2013.08.035>.
- 6 [112] W. Qiang, W.-M. Yau, Y. Luo, M.P. Mattson, R. Tycko, Antiparallel β -sheet architecture
7 in Iowa-mutant β -amyloid fibrils, *Proc. Natl. Acad. Sci.* 109 (2012) 4443–4448.
8 <https://doi.org/10.1073/pnas.1111305109>.
- 9 [113] A.K. Paravastu, R.D. Leapman, W.-M. Yau, R. Tycko, Molecular structural basis for
10 polymorphism in Alzheimer's β -amyloid fibrils, *Proc. Natl. Acad. Sci.* 105 (2008)
11 18349–18354. <https://doi.org/10.1073/pnas.0806270105>.
- 12 [114] C. Sachse, M. Fändrich, N. Grigorieff, Paired β -sheet structure of an A β (1-40) amyloid
13 fibril revealed by electron microscopy, *Proc. Natl. Acad. Sci. U. S. A.* 105 (2008) 7462–
14 7466. <https://doi.org/10.1073/pnas.0712290105>.
- 15 [115] C. Sachse, N. Grigorieff, M. Fändrich, Nanoscale flexibility parameters of Alzheimer
16 amyloid fibrils determined by electron cryo-microscopy, *Angew. Chem. Int. Ed Engl.*
17 49 (2010) 1321–1323. <https://doi.org/10.1002/anie.200904781>.
- 18 [116] M. Schmidt, C. Sachse, W. Richter, C. Xu, M. Fändrich, N. Grigorieff, Comparison of
19 Alzheimer A β (1–40) and A β (1–42) amyloid fibrils reveals similar protofilament
20 structures, *Proc. Natl. Acad. Sci.* 106 (2009) 19813–19818.
21 <https://doi.org/10.1073/pnas.0905007106>.
- 22 [117] L. Gremer, D. Schölzel, C. Schenk, E. Reinartz, J. Labahn, R.B.G. Ravelli, M. Tusche, C.
23 Lopez-Iglesias, W. Hoyer, H. Heise, D. Willbold, G.F. Schröder, Fibril structure of

- 1 amyloid- β (1–42) by cryo–electron microscopy, *Science*. 358 (2017) 116–119.
2 <https://doi.org/10.1126/science.aao2825>.
- 3 [118] M.A. Wälti, F. Ravotti, H. Arai, C.G. Glabe, J.S. Wall, A. Böckmann, P. Güntert, B.H.
4 Meier, R. Riek, Atomic-resolution structure of a disease-relevant A β (1–42) amyloid
5 fibril, *Proc. Natl. Acad. Sci.* 113 (2016) E4976–E4984.
6 <https://doi.org/10.1073/pnas.1600749113>.
- 7 [119] M.T. Colvin, R. Silvers, Q.Z. Ni, T.V. Can, I. Sergeev, M. Rosay, K.J. Donovan, B.
8 Michael, J. Wall, S. Linse, R.G. Griffin, Atomic resolution structure of monomorphic
9 A β ₄₂ amyloid fibrils, *J. Am. Chem. Soc.* 138 (2016) 9663–9674.
10 <https://doi.org/10.1021/jacs.6b05129>.
- 11 [120] M. Schmidt, A. Rohou, K. Lasker, J.K. Yadav, C. Schiene-Fischer, M. Fändrich, N.
12 Grigorieff, Peptide dimer structure in an A β (1–42) fibril visualized with cryo-EM, *Proc.*
13 *Natl. Acad. Sci.* 112 (2015) 11858–11863. <https://doi.org/10.1073/pnas.1503455112>.
- 14 [121] Y. Xiao, B. Ma, D. McElheny, S. Parthasarathy, F. Long, M. Hoshi, R. Nussinov, Y. Ishii,
15 A β (1–42) fibril structure illuminates self-recognition and replication of amyloid in
16 Alzheimer’s disease, *Nat. Struct. Mol. Biol.* 22 (2015) 499–505.
17 <https://doi.org/10.1038/nsmb.2991>.
- 18 [122] R. Zhang, X. Hu, H. Khant, S.J. Ludtke, W. Chiu, M.F. Schmid, C. Frieden, J.-M. Lee,
19 Interprotofilament interactions between Alzheimer’s A β _{1–42} peptides in amyloid fibrils
20 revealed by cryoEM, *Proc. Natl. Acad. Sci.* 106 (2009) 4653–4658.
21 <https://doi.org/10.1073/pnas.0901085106>.
- 22 [123] T. Lührs, C. Ritter, M. Adrian, D. Riek-Loher, B. Bohrmann, H. Döbeli, D. Schubert, R.
23 Riek, 3D structure of Alzheimer’s amyloid- β (1–42) fibrils, *Proc. Natl. Acad. Sci.* 102
24 (2005) 17342–17347. <https://doi.org/10.1073/pnas.0506723102>.

- 1 [124] K. Zhao, Y.-J. Lim, Z. Liu, H. Long, Y. Sun, J.-J. Hu, C. Zhao, Y. Tao, X. Zhang, D. Li, Y.-M.
2 Li, C. Liu, Parkinson's disease-related phosphorylation at Tyr39 rearranges α -synuclein
3 amyloid fibril structure revealed by cryo-EM, *Proc. Natl. Acad. Sci.* 117 (2020) 20305–
4 20315. <https://doi.org/10.1073/pnas.1922741117>.
- 5 [125] K. Zhao, Y. Li, Z. Liu, H. Long, C. Zhao, F. Luo, Y. Sun, Y. Tao, X. Su, D. Li, X. Li, C. Liu,
6 Parkinson's disease associated mutation E46K of α -synuclein triggers the formation of
7 a distinct fibril structure, *Nat. Commun.* 11 (2020). [https://doi.org/10.1038/s41467-](https://doi.org/10.1038/s41467-020-16386-3)
8 020-16386-3.
- 9 [126] Y. Sun, S. Hou, K. Zhao, H. Long, Z. Liu, J. Gao, Y. Zhang, X.-D. Su, D. Li, C. Liu, Cryo-EM
10 structure of full-length α -synuclein amyloid fibril with Parkinson's disease familial
11 A53T mutation, *Cell Res.* 30 (2020) 360–362. [https://doi.org/10.1038/s41422-020-](https://doi.org/10.1038/s41422-020-0299-4)
12 0299-4.
- 13 [127] D.R. Boyer, B. Li, C. Sun, W. Fan, K. Zhou, M.P. Hughes, M.R. Sawaya, L. Jiang, D.S.
14 Eisenberg, The α -synuclein hereditary mutation E46K unlocks a more stable,
15 pathogenic fibril structure, *Proc. Natl. Acad. Sci.* 117 (2020) 3592–3602.
16 <https://doi.org/10.1073/pnas.1917914117>.
- 17 [128] M. Schweighauser, Y. Shi, A. Tarutani, F. Kametani, A.G. Murzin, B. Ghetti, T.
18 Matsubara, T. Tomita, T. Ando, K. Hasegawa, S. Murayama, M. Yoshida, M. Hasegawa,
19 S.H.W. Scheres, M. Goedert, Structures of α -synuclein filaments from multiple system
20 atrophy, *Nature.* 585 (2020) 464–469. <https://doi.org/10.1038/s41586-020-2317-6>.
- 21 [129] R. Guerrero-Ferreira, N.M. Taylor, A.-A. Arteni, P. Kumari, D. Mona, P. Ringler, M.
22 Britschgi, M.E. Lauer, A. Makky, J. Verasdonck, R. Riek, R. Melki, B.H. Meier, A.
23 Böckmann, L. Bousset, H. Stahlberg, Two new polymorphic structures of human full-

- 1 length alpha-synuclein fibrils solved by cryo-electron microscopy, *ELife*. 8 (2019)
2 e48907. <https://doi.org/10.7554/eLife.48907>.
- 3 [130] D.R. Boyer, B. Li, C. Sun, W. Fan, M.R. Sawaya, L. Jiang, D.S. Eisenberg, Structures of
4 fibrils formed by α -synuclein hereditary disease mutant H50Q reveal new
5 polymorphs, *Nat. Struct. Mol. Biol.* 26 (2019) 1044–1052.
6 <https://doi.org/10.1038/s41594-019-0322-y>.
- 7 [131] X. Ni, R.P. McGlinchey, J. Jiang, J.C. Lee, Structural insights into α -synuclein fibril
8 polymorphism: Effects of Parkinson’s disease-related C-terminal truncations, *J. Mol.*
9 *Biol.* 431 (2019) 3913–3919. <https://doi.org/10.1016/j.jmb.2019.07.001>.
- 10 [132] B. Li, P. Ge, K.A. Murray, P. Sheth, M. Zhang, G. Nair, M.R. Sawaya, W.S. Shin, D.R.
11 Boyer, S. Ye, D.S. Eisenberg, Z.H. Zhou, L. Jiang, Cryo-EM of full-length α -synuclein
12 reveals fibril polymorphs with a common structural kernel, *Nat. Commun.* 9 (2018)
13 3609. <https://doi.org/10.1038/s41467-018-05971-2>.
- 14 [133] R. Guerrero-Ferreira, N.M. Taylor, D. Mona, P. Ringler, M.E. Lauer, R. Riek, M.
15 Britschgi, H. Stahlberg, Cryo-EM structure of alpha-synuclein fibrils, *ELife*. 7 (2018)
16 e36402. <https://doi.org/10.7554/eLife.36402>.
- 17 [134] Y. Li, C. Zhao, F. Luo, Z. Liu, X. Gui, Z. Luo, X. Zhang, D. Li, C. Liu, X. Li, Amyloid fibril
18 structure of α -synuclein determined by cryo-electron microscopy, *Cell Res.* (2018) 1.
19 <https://doi.org/10.1038/s41422-018-0075-x>.
- 20 [135] M.D. Tuttle, G. Comellas, A.J. Nieuwkoop, D.J. Covell, D.A. Berthold, K.D. Kloepper,
21 J.M. Courtney, J.K. Kim, A.M. Barclay, A. Kendall, W. Wan, G. Stubbs, C.D. Schwieters,
22 V.M.Y. Lee, J.M. George, C.M. Rienstra, Solid-state NMR structure of a pathogenic
23 fibril of full-length human α -synuclein, *Nat. Struct. Mol. Biol.* 23 (2016) 409–415.
24 <https://doi.org/10.1038/nsmb.3194>.

- 1 [136] A.D. Dearborn, J.S. Wall, N. Cheng, J.B. Heymann, A.V. Kajava, J. Varkey, R. Langen,
2 A.C. Steven, α -synuclein amyloid fibrils with two entwined, asymmetrically associated
3 protofibrils, *J. Biol. Chem.* 291 (2016) 2310–2318.
4 <https://doi.org/10.1074/jbc.M115.698787>.
- 5 [137] C. Seuring, J. Verasdonck, J. Gath, D. Ghosh, N. Nespovitaya, M.A. Wälti, S.K. Maji, R.
6 Cadalbert, P. Güntert, B.H. Meier, R. Riek, The three-dimensional structure of human
7 β -endorphin amyloid fibrils, *Nat. Struct. Mol. Biol.* 27 (2020) 1178–1184.
8 <https://doi.org/10.1038/s41594-020-00515-z>.
- 9 [138] M.G. Iadanza, R. Silvers, J. Boardman, H.I. Smith, T.K. Karamanos, G.T. Debelouchina,
10 Y. Su, R.G. Griffin, N.A. Ranson, S.E. Radford, The structure of a β 2-microglobulin fibril
11 suggests a molecular basis for its amyloid polymorphism, *Nat. Commun.* 9 (2018)
12 4517. <https://doi.org/10.1038/s41467-018-06761-6>.
- 13 [139] K. Iwata, T. Fujiwara, Y. Matsuki, H. Akutsu, S. Takahashi, H. Naiki, Y. Goto, 3D
14 structure of amyloid protofilaments of β 2-microglobulin fragment probed by solid-
15 state NMR, *Proc. Natl. Acad. Sci.* 103 (2006) 18119–18124.
16 <https://doi.org/10.1073/pnas.0607180103>.
- 17 [140] N. Ferguson, J. Becker, H. Tidow, S. Tremmel, T.D. Sharpe, G. Krause, J. Flinders, M.
18 Petrovich, J. Berriman, H. Oschkinat, A.R. Fersht, General structural motifs of amyloid
19 protofilaments, *Proc. Natl. Acad. Sci.* 103 (2006) 16248–16253.
20 <https://doi.org/10.1073/pnas.0607815103>.
- 21 [141] M. Lee, U. Ghosh, K.R. Thurber, M. Kato, R. Tycko, Molecular structure and
22 interactions within amyloid-like fibrils formed by a low-complexity protein sequence
23 from FUS, *Nat. Commun.* 11 (2020) 5735. [https://doi.org/10.1038/s41467-020-19512-](https://doi.org/10.1038/s41467-020-19512-3)
24 3.

- 1 [142] M.D. Gelenter, K.J. Smith, S.-Y. Liao, V.S. Mandala, A.J. Dregni, M.S. Lamm, Y. Tian, W.
2 Xu, D.J. Pochan, T.J. Tucker, Y. Su, M. Hong, The peptide hormone glucagon forms
3 amyloid fibrils with two coexisting β -strand conformations, *Nat. Struct. Mol. Biol.* 26
4 (2019) 592–598. <https://doi.org/10.1038/s41594-019-0238-6>.
- 5 [143] U.S. Herrmann, A.K. Schütz, H. Shirani, D. Huang, D. Saban, M. Nuvolone, B. Li, B.
6 Ballmer, A.K.O. Åslund, J.J. Mason, E. Rushing, H. Budka, S. Nyström, P.
7 Hammarström, A. Böckmann, A. Caflich, B.H. Meier, K.P.R. Nilsson, S. Hornemann, A.
8 Aguzzi, Structure-based drug design identifies polythiophenes as antiprion
9 compounds, *Sci. Transl. Med.* 7 (2015) 299ra123-299ra123.
10 <https://doi.org/10.1126/scitranslmed.aab1923>.
- 11 [144] A.K. Schütz, A. Soragni, S. Hornemann, A. Aguzzi, M. Ernst, A. Böckmann, B.H. Meier,
12 The amyloid–Congo red Interface at atomic resolution, *Angew. Chem. Int. Ed.* 50
13 (2011) 5956–5960. <https://doi.org/10.1002/anie.201008276>.
- 14 [145] N. Mizuno, U. Baxa, A.C. Steven, Structural dependence of HET-s amyloid fibril
15 infectivity assessed by cryoelectron microscopy, *Proc. Natl. Acad. Sci.* 108 (2011)
16 3252–3257. <https://doi.org/10.1073/pnas.1011342108>.
- 17 [146] H. Van Melckebeke, C. Wasmer, A. Lange, E. AB, A. Loquet, A. Böckmann, B.H. Meier,
18 Atomic-resolution three-dimensional structure of HET-s(218–289) amyloid fibrils by
19 solid-state NMR spectroscopy, *J. Am. Chem. Soc.* 132 (2010) 13765–13775.
20 <https://doi.org/10.1021/ja104213j>.
- 21 [147] C. Wasmer, A. Lange, H. Van Melckebeke, A.B. Siemer, R. Riek, B.H. Meier, Amyloid
22 fibrils of the HET-s(218-289) prion form a β solenoid with a triangular hydrophobic
23 core, *Science.* 319 (2008) 1523–1526. <https://doi.org/10.1126/science.1151839>.

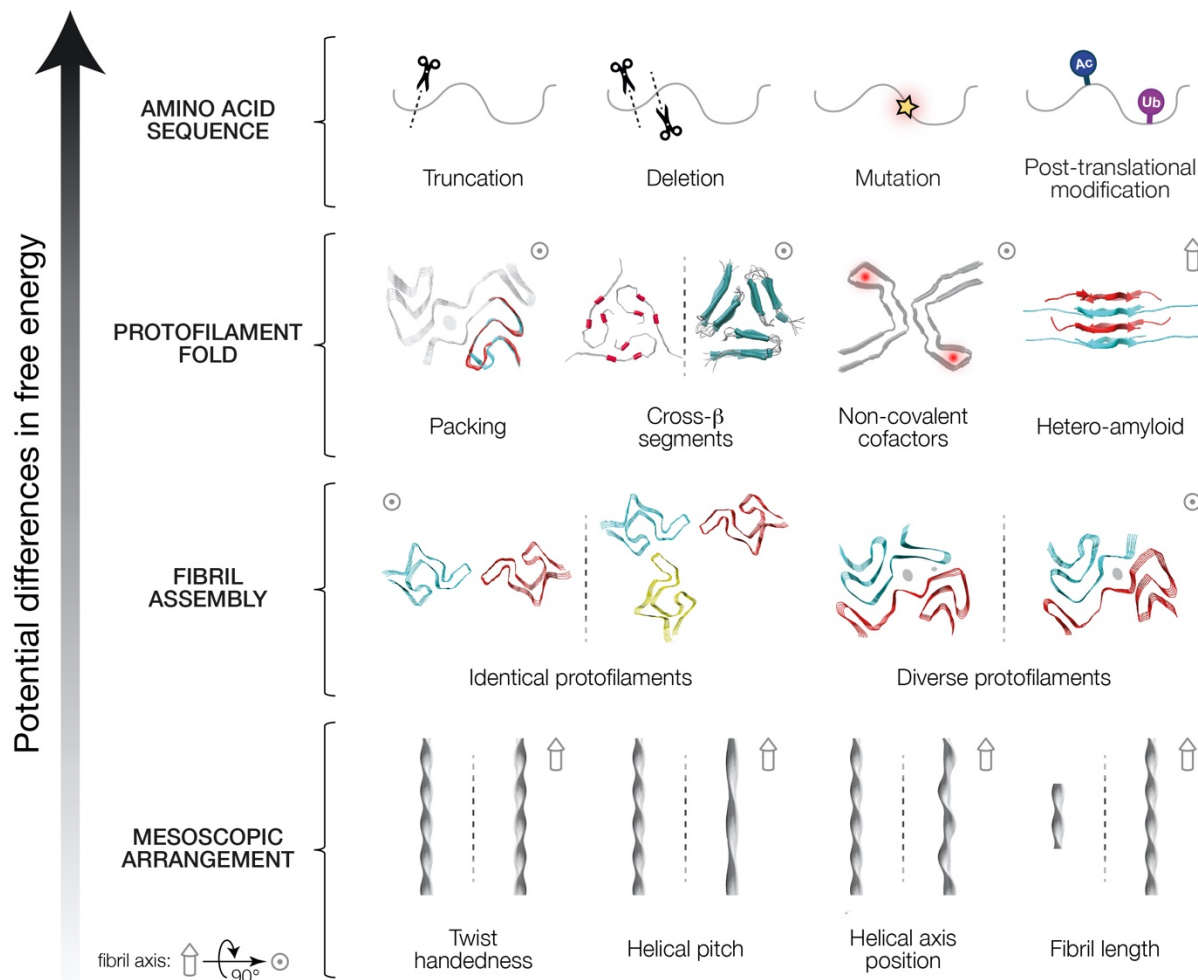
- 1 [148] Y. Sun, K. Zhao, W. Xia, G. Feng, J. Gu, Y. Ma, X. Gui, X. Zhang, Y. Fang, B. Sun, R.
2 Wang, C. Liu, D. Li, The nuclear localization sequence mediates hnRNPA1 amyloid
3 fibril formation revealed by cryoEM structure, *Nat. Commun.* 11 (2020) 6349.
4 <https://doi.org/10.1038/s41467-020-20227-8>.
- 5 [149] Q. Cao, D.R. Boyer, M.R. Sawaya, P. Ge, D.S. Eisenberg, Cryo-EM structure and
6 inhibitor design of human IAPP (amylin) fibrils, *Nat. Struct. Mol. Biol.* 27 (2020) 653–
7 659. <https://doi.org/10.1038/s41594-020-0435-3>.
- 8 [150] C. Röder, T. Kupreichyk, L. Gremer, L.U. Schäfer, K.R. Pothula, R.B.G. Ravelli, D.
9 Willbold, W. Hoyer, G.F. Schröder, Cryo-EM structure of islet amyloid polypeptide
10 fibrils reveals similarities with amyloid- β fibrils, *Nat. Struct. Mol. Biol.* 27 (2020) 660–
11 667. <https://doi.org/10.1038/s41594-020-0442-4>.
- 12 [151] W. Close, M. Neumann, A. Schmidt, M. Hora, K. Annamalai, M. Schmidt, B. Reif, V.
13 Schmidt, N. Grigorieff, M. Fändrich, Physical basis of amyloid fibril polymorphism,
14 *Nat. Commun.* 9 (2018) 699. <https://doi.org/10.1038/s41467-018-03164-5>.
- 15 [152] A. Schmidt, K. Annamalai, M. Schmidt, N. Grigorieff, M. Fändrich, Cryo-EM reveals the
16 steric zipper structure of a light chain-derived amyloid fibril, *Proc. Natl. Acad. Sci.* 113
17 (2016) 6200–6205. <https://doi.org/10.1073/pnas.1522282113>.
- 18 [153] C. Röder, N. Vettore, L.N. Mangels, L. Gremer, R.B.G. Ravelli, D. Willbold, W. Hoyer,
19 A.K. Buell, G.F. Schröder, Atomic structure of PI3-kinase SH3 amyloid fibrils by cryo-
20 electron microscopy, *Nat. Commun.* 10 (2019) 3754. [https://doi.org/10.1038/s41467-
21 019-11320-8](https://doi.org/10.1038/s41467-019-11320-8).
- 22 [154] L.-Q. Wang, K. Zhao, H.-Y. Yuan, Q. Wang, Z. Guan, J. Tao, X.-N. Li, Y. Sun, C.-W. Yi, J.
23 Chen, D. Li, D. Zhang, P. Yin, C. Liu, Y. Liang, Cryo-EM structure of an amyloid fibril

- 1 formed by full-length human prion protein, *Nat. Struct. Mol. Biol.* 27 (2020) 598–602.
2 <https://doi.org/10.1038/s41594-020-0441-5>.
- 3 [155] C. Glynn, M.R. Sawaya, P. Ge, M. Gallagher-Jones, C.W. Short, R. Bowman, M. Apostol,
4 Z.H. Zhou, D.S. Eisenberg, J.A. Rodriguez, Cryo-EM structure of a human prion fibril
5 with a hydrophobic, protease-resistant core, *Nat. Struct. Mol. Biol.* 27 (2020) 417–
6 423. <https://doi.org/10.1038/s41594-020-0403-y>.
- 7 [156] M. Mompeán, W. Li, J. Li, S. Laage, A.B. Siemer, G. Bozkurt, H. Wu, A.E. McDermott,
8 The structure of the necrosome RIPK1-RIPK3 core, a human hetero-amyloid signaling
9 complex, *Cell.* 173 (2018) 1244-1253.e10. <https://doi.org/10.1016/j.cell.2018.03.032>.
- 10 [157] X.-L. Wu, H. Hu, X.-Q. Dong, J. Zhang, J. Wang, C.D. Schwieters, J. Liu, G.-X. Wu, B. Li,
11 J.-Y. Lin, H.-Y. Wang, J.-X. Lu, The amyloid structure of mouse RIPK3 (receptor
12 interacting protein kinase 3) in cell necroptosis, *Nat. Commun.* 12 (2021) 1627.
13 <https://doi.org/10.1038/s41467-021-21881-2>.
- 14 [158] F. Liberta, S. Loerch, M. Rennegarbe, A. Schierhorn, P. Westermark, G.T. Westermark,
15 B.P.C. Hazenberg, N. Grigorieff, M. Fändrich, M. Schmidt, Cryo-EM fibril structures
16 from systemic AA amyloidosis reveal the species complementarity of pathological
17 amyloids, *Nat. Commun.* 10 (2019) 1104. [https://doi.org/10.1038/s41467-019-09033-](https://doi.org/10.1038/s41467-019-09033-z)
18 z.
- 19 [159] Q. Li, W.M. Babinchak, W.K. Surewicz, Cryo-EM structure of amyloid fibrils formed by
20 the entire low complexity domain of TDP-43, *Nat. Commun.* 12 (2021) 1620.
21 <https://doi.org/10.1038/s41467-021-21912-y>.
- 22 [160] Q. Cao, D.R. Boyer, M.R. Sawaya, P. Ge, D.S. Eisenberg, Cryo-EM structures of four
23 polymorphic TDP-43 amyloid cores, *Nat. Struct. Mol. Biol.* 26 (2019) 619–627.
24 <https://doi.org/10.1038/s41594-019-0248-4>.

- 1 [161] E.L. Guenther, P. Ge, H. Trinh, M.R. Sawaya, D. Cascio, D.R. Boyer, T. Gonen, Z.H.
2 Zhou, D.S. Eisenberg, Atomic-level evidence for packing and positional amyloid
3 polymorphism by segment from TDP-43 RRM2, *Nat. Struct. Mol. Biol.* 25 (2018) 311–
4 319. <https://doi.org/10.1038/s41594-018-0045-5>.
- 5 [162] M. Schmidt, S. Wiese, V. Adak, J. Engler, S. Agarwal, G. Fritz, P. Westermark, M.
6 Zacharias, M. Fändrich, Cryo-EM structure of a transthyretin-derived amyloid fibril
7 from a patient with hereditary ATTR amyloidosis, *Nat. Commun.* 10 (2019) 5008.
8 <https://doi.org/10.1038/s41467-019-13038-z>.
- 9 [163] C.P. Jaroniec, C.E. MacPhee, V.S. Bajaj, M.T. McMahon, C.M. Dobson, R.G. Griffin,
10 High-resolution molecular structure of a peptide in an amyloid fibril determined by
11 magic angle spinning NMR spectroscopy, *Proc. Natl. Acad. Sci.* 101 (2004) 711–716.
12 <https://doi.org/10.1073/pnas.0304849101>.
- 13
14
15

1 Figure legends

2



3

4

5 **Figure 1. Hierarchical structural polymorphism of amyloid fibrils.** Top row: Modifications

6 of the primary amino acid sequence, including truncations, deletions, mutations, and post-

7 translational modifications, represent the first layer of complexity that leads to the diversity of

8 amyloid structures. Second row: Polypeptide chains with identical amino acid sequences may

9 exhibit further differences in the adopted protofilament fold upon assembly, including

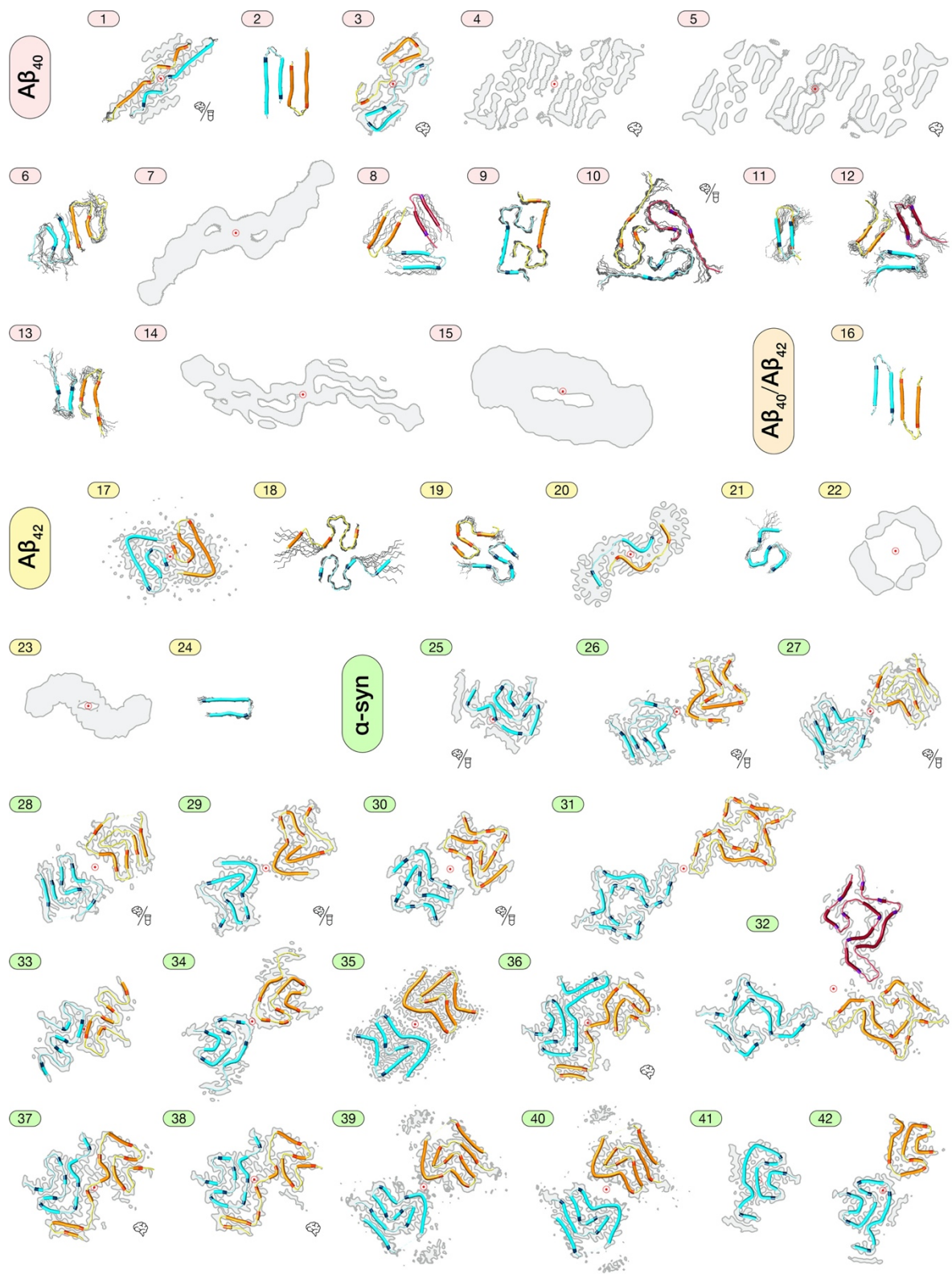
10 differences in the β -sheet forming regions (segmental polymorphism; demonstrated by $A\beta_{40}$

11 PDB IDs 2M4J and 2LMQ on the left and right, respectively), the arrangement of the core fold

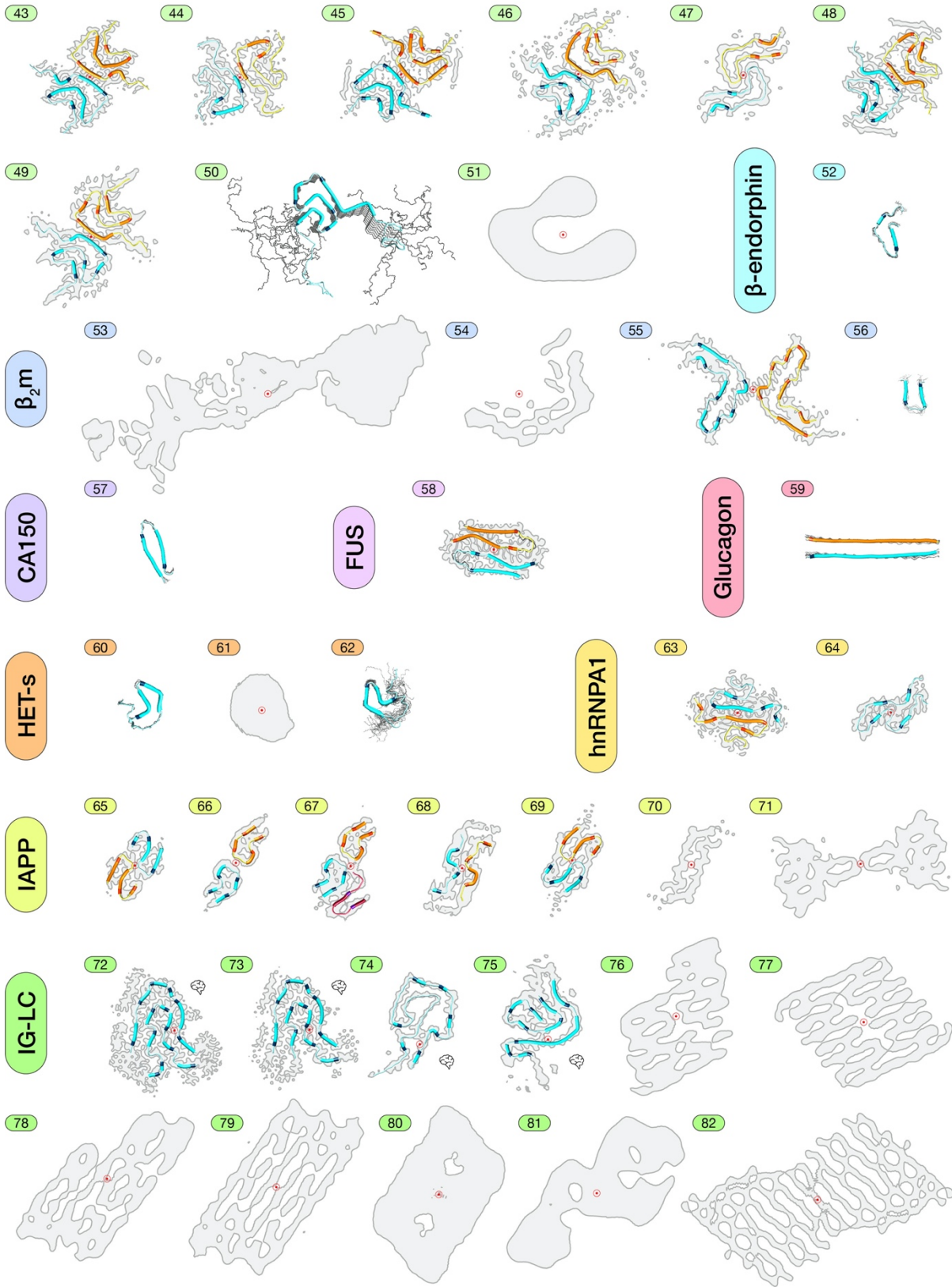
12 (packing polymorphism; demonstrated by overlay of α -synuclein PDB IDs 6XYP and 6XYQ)

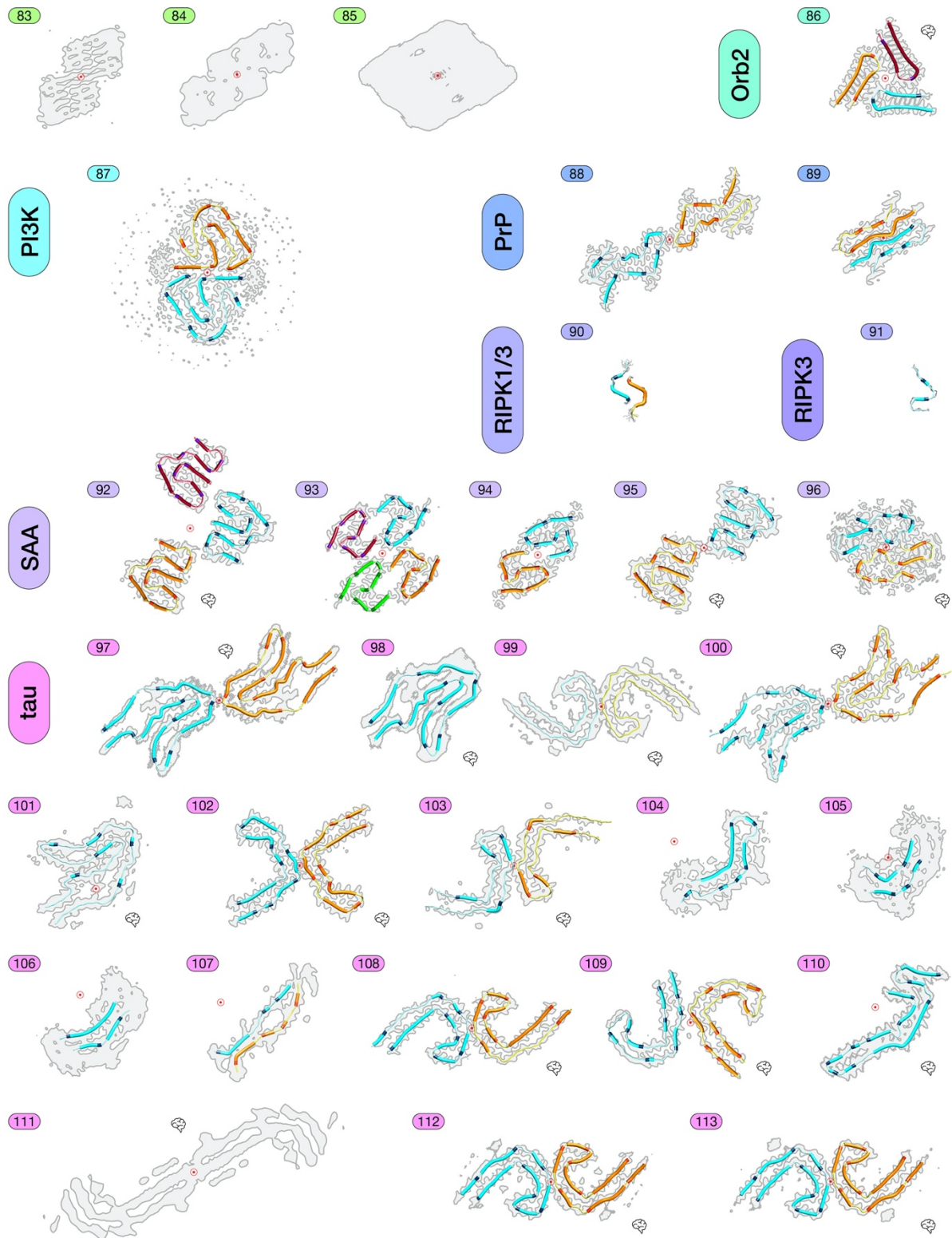
1 and the presence of noncovalent co-factors (tau PDB ID 6NWP). Interestingly, heteroamyloid
2 can result from alternate stacking of monomers with different sequences to form a fibril
3 (RIPK1/3 PDB ID 5V7Z). Third row: Assembly of identical or different protofilaments by
4 lateral associations can result in further diversity of amyloid structures. Assembly
5 polymorphism with identical folds is illustrated by α -synuclein PDB IDs 6L1T (left) and 6L1U
6 (right) and for fibrils with diverse folds the accession codes are 6XYO (left) and 6XYP (right),
7 also showing α -synuclein fibrils. Bottom row: Polymorphism can also arise in the mesoscopic
8 length scale from differences in twist handedness, helical pitch, the position of the helical axis
9 and the number of monomers in the fibril, which determines the length. Molecular models were
10 generated using UCSF Chimera [104].

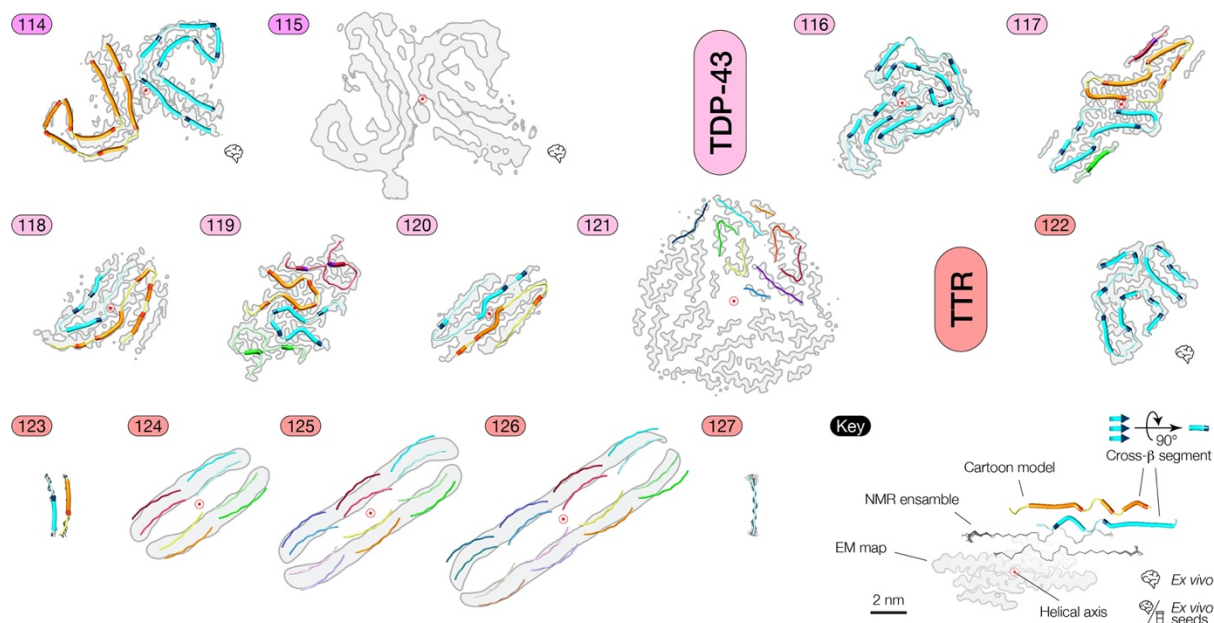
11



1

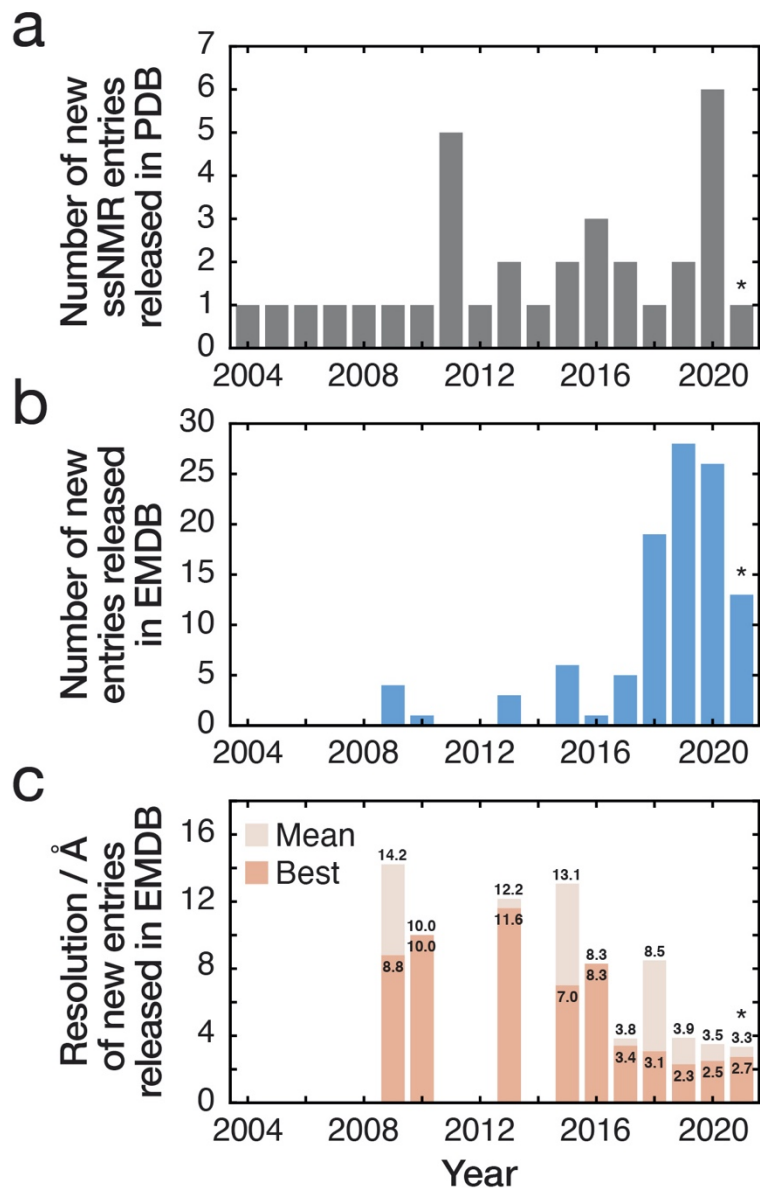






1
2 **Figure 2. Diversity of cross- β structures demonstrated by a graphical summary of**
3 **structural data of amyloid fibrils acquired by cryo-EM or ssNMR.** Average cross-section
4 of cryo-EM density maps, ssNMR ensembles, and structural models of amyloid fibrils
5 containing constituent polypeptide segments longer than 10 amino acids deposited in the
6 EMDB and PDB databases up until March 2021 are shown in an orientation with the fibril axis
7 perpendicular to the page plane. The entries are grouped by protein name and then by the
8 release date of the data entry, with the newest data entry shown first. The numbers shown
9 correspond to the entry numbers listed in Table 2. Structural models are displayed by a coloured
10 ribbon representation in cases where PDB entries are available. Each polypeptide chain in the
11 cross-section view is coloured differently, with the cross- β segments, where such segments are
12 determined and labelled in the PDB entry, shown as a wider chains in a darker shade and their
13 C-terminal residues shown in an even darker shade. A single layer of each fibril model along
14 the helical axis is shown only, for clarity. For ssNMR ensembles, the first model is shown in
15 the coloured ribbon representation and other models are shown in grey wire representation.
16 Cryo-EM maps are shown as grey average cross-sections with a darker grey outline

1 representing the iso-line that defines the density boundary. The cross-sections were drawn by
2 first untwisting the map to a single slice along the length of the fibril using published twist and
3 rise values, and isolines were subsequently generated using the recommended isovalue
4 provided by the authors in the EMDB entry. A key is provided in the bottom right corner of
5 the figure, showing the cartoon labels for entries of *ex vivo* samples or of *ex vivo* seeded
6 samples used throughout. All models and representations are scaled equally, with the scale bar
7 representing the length of 20 Å. Molecular models were generated using UCSF Chimera [104].
8
9

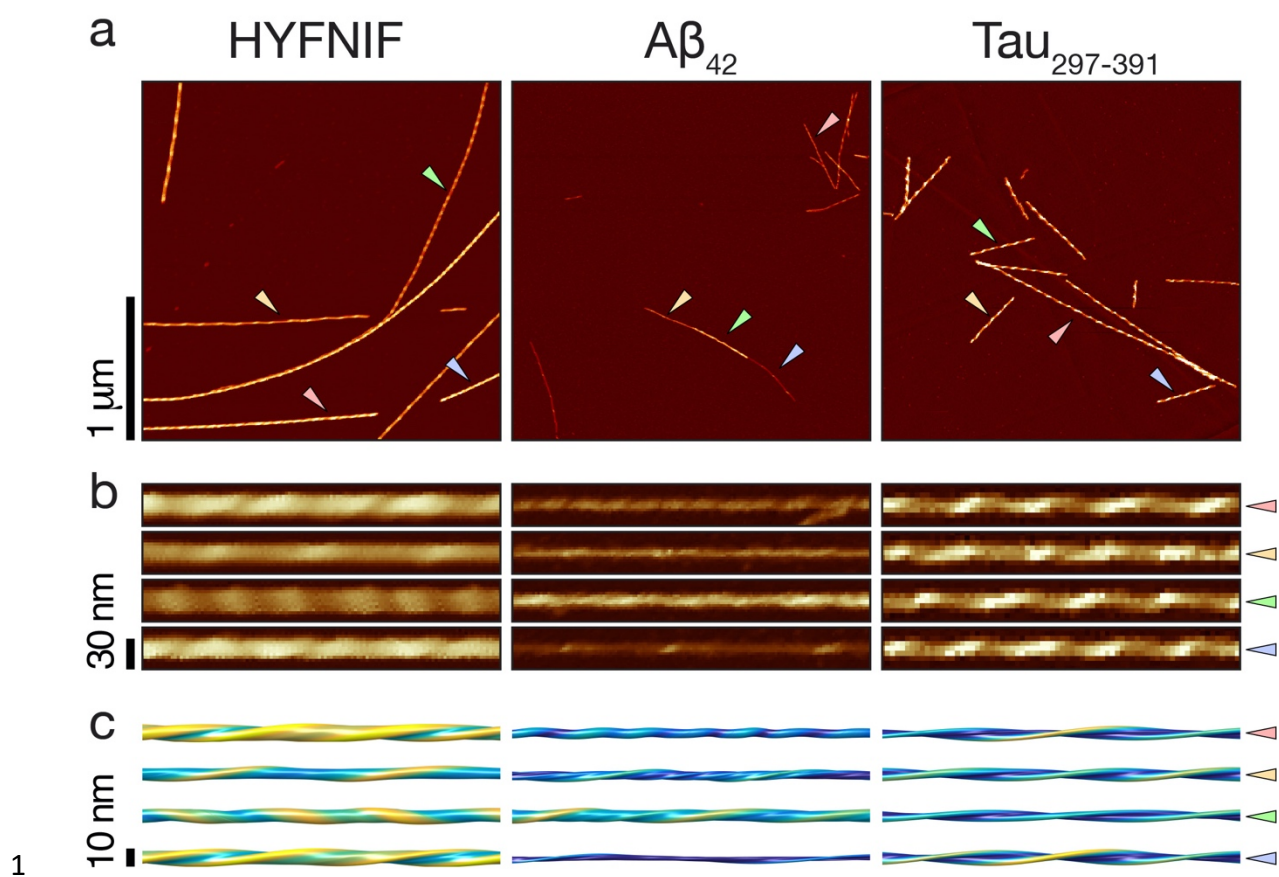


1

2 **Figure 3. The number of structural data entries of amyloid fibrils deposited to the EMDB**
 3 **and PDB databases is rapidly growing, and the resolution of cryo-EM data is improving.**

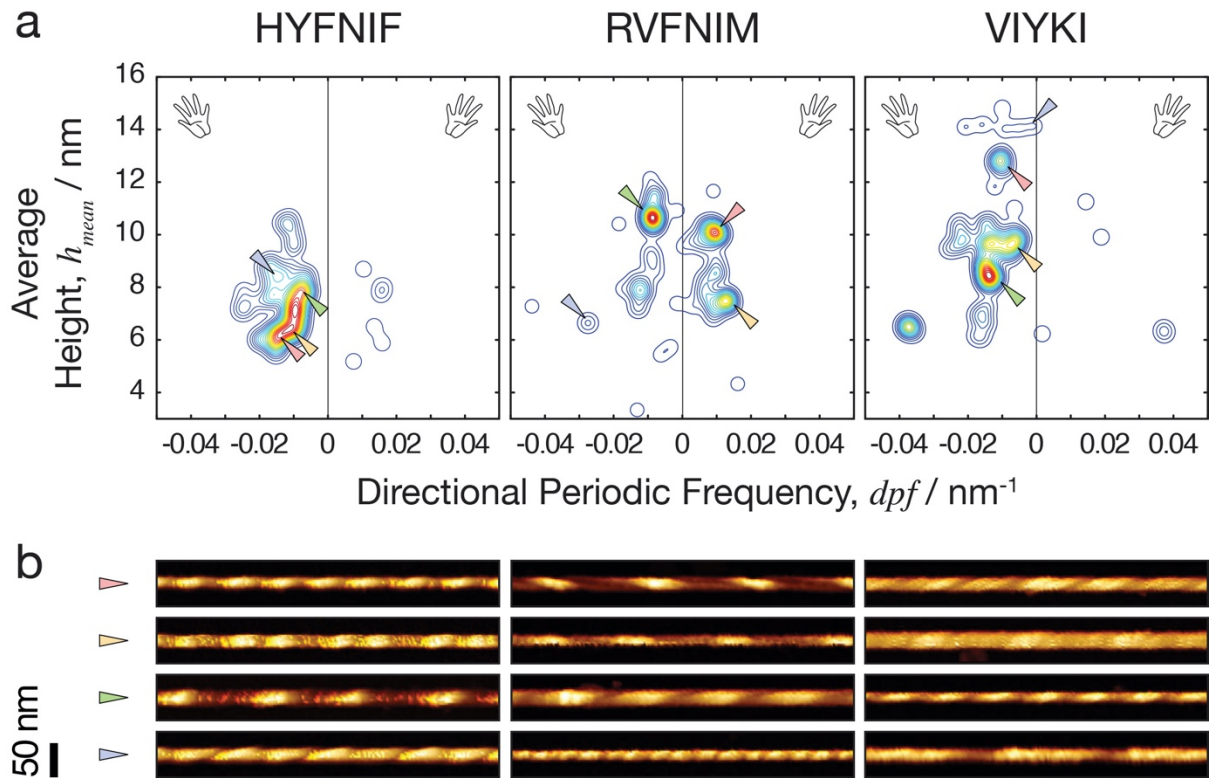
4 a) Number of new amyloid structural models determined by ssNMR deposited to the PDB
 5 released each year since 2004. b) Number of new amyloid cryo-EM data deposited to the
 6 EMDB released each year since 2009. c) Mean and best resolutions of cryo-EM data of amyloid
 7 fibrils each year. The star symbols (*) indicate that only entries released up until March are
 8 included for 2021.

9



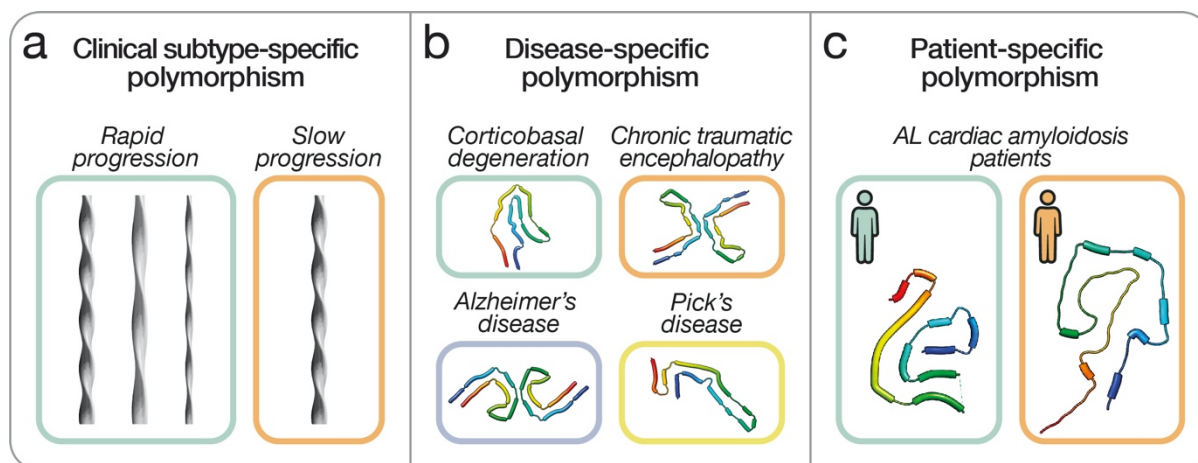
1
2 **Figure 4. Structural details individual to each amyloid fibril are revealed by AFM.** Gentle
3 force-distance curve-based AFM imaging and 3D-reconstruction of fibril surface envelopes
4 revealed the individuality of amyloid fibrils in amyloid populations, with no two fibrils being
5 exactly the same. a) AFM height topology images of amyloid fibrils formed from a hexa-
6 peptide of the primary sequence HYFNIF [25], Aβ₄₂, and a tau₂₉₇₋₃₉₁ fragment (also called dGAE)
7 [58]. The images are shown with the same length and colour scale, with the scale bar to the left
8 indicating the length of 1 μm in all three images. b) Images of digitally straightened fibrils seen
9 in the images in a), with the coloured triangle markers indicating their position in a). A 350 nm
10 segment of each fibril is shown. c) The 3D surface envelope models individually reconstructed
11 for each fibril in b) are shown with surface colours ranging from blue to yellow to indicate the
12 distance to the fibril axis from thin to wide. A 200 nm segment of each 3D model is shown.
13 These AFM images and individual fibril models suggest that the extent of structural
14 polymorphism is not the same for different amyloid forming sequences, with fibrils formed

- 1 from tau₂₉₇₋₃₉₁ showing the least extent of polymorphism amongst the three examples.
- 2 Polymorphic structural variation within a fibril is also seen on the image of A β ₄₂ fibrils.
- 3
- 4



1
2 **Figure 5. Structural analysis of individual fibrils using AFM allows mapping of the**
3 **polymorphic amyloid assembly landscape.** a) The polymorphic amyloid assembly
4 landscapes of three short amyloid forming peptide sequences are represented as smoothed 2D
5 histograms and visualised as contour maps [25]. The colouring represents the density of the
6 morphometric parameters, which include the average height and the number of repeating units
7 per nm (directional periodic frequency, dpf) of the individual fibrils observed on AFM height
8 images. Negative and positive dpf values correspond to fibrils with left-handed twist and right-
9 handed twist, respectively. b) Example images of digitally straightened fibrils formed from the
10 three peptide sequences in a), with the coloured triangle markers indicating their position in
11 the maps in a). A 500 nm segment of each fibril is shown.

12



1
2 **Figure 6. Amyloid polymorphism shows diverse patterns in disease-states.** a) Illustrations
3 of the varying extent of structural polymorphism and the diverse types of polymorphic
4 structures that may be present in clinical disease subtypes, for example shown for rapid and
5 slow progressive Alzheimer's disease [93,94]. b) Disease-specific polymorphism has been
6 demonstrated for amyloid structures formed from tau protein in various tauopathies. A single
7 representative cartoon model is shown of amyloid fibril cross-sections from samples
8 originating from the brain tissue of patients with four different neurodegenerative diseases,
9 with the thicker sections denoting the cross- β segments, where such segments are determined
10 and labelled in the PDB entry. PDB accession codes for the models shown are 6VHA, 6NWP,
11 5O3L and 6GX5 [13,15,38,91], for chronic corticobasal degeneration, traumatic
12 encephalopathy, Alzheimer's disease, and Pick's disease, respectively. c) Individual patients
13 with the same diagnosis may have distinct structures of the same protein, for example in the
14 case of AL amyloidosis. Cartoon models of the cross-sections of *ex vivo* amyloid fibrils
15 extracted from the cardiac tissue of two patients with AL amyloidosis are shown, with PDB
16 accession codes 6HUD and 6IC3 [98,99], respectively. Molecular models were generated using
17 UCSF Chimera [104].

18
19

1

2 **Table 1. Summary of experimental techniques for 3D structural characterisation of**
 3 **polymorphic amyloid fibrils.** Data type and structural information obtainable from the three
 4 methods highlighted in this review, i.e., cryo-electron microscopy (cryo-EM), solid-state
 5 nuclear magnetic resonance spectroscopy (ssNMR), and atomic force microscopy (AFM), are
 6 described.

	Cryo-EM	ssNMR	AFM
Data type	Projection images/transmission electron micrographs	Resonance frequencies/chemical shifts of atomic nuclei	Surface topography (height) images
Structural information	3D coulomb potential maps	Atomic distances, bond angles, and local chemical environment information	3D molecular surface envelopes
Features	Can provide high-resolution (<4Å) averaged structural maps	Generates an ensemble of possible molecular models	Can provide individual particle information and allows collection of nano-mechanical or chemical information

7

1 **Table 2. Three-dimensional structural data entries of amyloid fibrils acquired by cryo-**
2 **EM or ssNMR.** Entries that are released in the EMDB and PDB databases running up to March
3 2021 are shown.

	Amyloid name *	Sample origin §	Experimental method	PDB ID ‡	EMDB ID †	Release date	Reference
1	A β _o	AD brain, seeded	ssNMR & cryo-EM	6w0o	21501	13/01/2021	[105]
2	A β _o		ssNMR	6ti5		22/07/2020	[106]
3	A β _o	AD brain	cryo-EM	6shs	10204	06/11/2019	[56]
4	A β _o	AD brain	cryo-EM		4864	06/11/2019	
5	A β _o	AD brain	cryo-EM		4866	06/11/2019	
6	A β _o		ssNMR	6oc9		05/06/2019	[107]
7	A β _o		cryo-EM		6326, 6327, 6328	29/04/2015	[108]
8	A β _o		ssNMR	2mpz		22/04/2015	[109]
9	A β _o		ssNMR	2mvx		26/11/2014	[110]
10	A β _o	AD brain, seeded	ssNMR	2m4j		25/09/2013	[111]
11	A β _o		ssNMR	2lnq		08/02/2012	[112]
12	A β _o		ssNMR	2lmq, 2lmp		28/12/2011	[113]
13	A β _o		ssNMR	2lmo, 2lmn		28/12/2011	
14	A β _o		cryo-EM		5008, 5132	08/10/2009	[114,115]
15	A β _o		cryo-EM		1650	24/09/2009	[116]
16	A β _o /A β _e		ssNMR	6ti6, 6ti7		22/07/2020	[106]
17	A β _e		cryo-EM	5oqv	3851	13/09/2017	[117]
18	A β _e		ssNMR	2nao		27/07/2016	[118]
19	A β _e		ssNMR	5kk3		13/07/2016	[119]
20	A β _e		cryo-EM	5aef	3132	26/08/2015	[120]
21	A β _e		ssNMR	2mxu		06/05/2015	[121]
22	A β _e		cryo-EM		5052	07/07/2010	[122]
23	A β _e		cryo-EM		1649	24/09/2009	[116]
24	A β _e		ssNMR	2beg		22/11/2005	[123]
25	α -syn	MSA brain, seeded	cryo-EM	7nck	12269	24/02/2021	[40]
26	α -syn	MSA brain, seeded	cryo-EM	7ncj	12268	24/02/2021	
27	α -syn	MSA brain, seeded	cryo-EM	7nci	12267	24/02/2021	
28	α -syn	MSA brain, seeded	cryo-EM	7nch	12266	24/02/2021	
29	α -syn	MSA brain, seeded	cryo-EM	7ncg	12265	24/02/2021	
30	α -syn	MSA brain, seeded	cryo-EM	7nca	12264	24/02/2021	
31	α -syn		cryo-EM	6l1t	0801	12/08/2020	[124]
32	α -syn		cryo-EM	6l1u	0803	12/08/2020	

33	α -syn		cryo-EM	6l4s	0833	29/04/2020	[125]
34	α -syn		cryo-EM	6lrq	0958	08/04/2020	[126]
35	α -syn		cryo-EM	6ufr	20759	19/02/2020	[127]
36	α -syn	MSA brain	cryo-EM	6xyo	10650	12/02/2020	[128]
37	α -syn	MSA brain	cryo-EM	6xyp	10651	12/02/2020	
38	α -syn	MSA brain	cryo-EM	6xyq	10652	12/02/2020	
39	α -syn		cryo-EM	6sst	10305	18/12/2019	[129]
40	α -syn		cryo-EM	6ssx	10307	18/12/2019	
41	α -syn		cryo-EM	6peo	20328	27/11/2019	[130]
42	α -syn		cryo-EM	6pes	20331	27/11/2019	
43	α -syn		cryo-EM	6osj	20183	25/09/2019	[131]
44	α -syn		cryo-EM	6osm	20186	25/09/2019	
45	α -syn		cryo-EM	6osl	20185	25/09/2019	
46	α -syn		cryo-EM	6cu7	7618	12/09/2018	[132]
47	α -syn		cryo-EM	6cu8	7619	12/09/2018	
48	α -syn		cryo-EM	6h6b	0148	08/08/2018	[133]
49	α -syn		cryo-EM	6a6b	0988	11/07/2018	[134]
50	α -syn		ssNMR	2n0a		23/03/2016	[135]
51	α -syn		cryo-EM		6482	16/12/2015	[136]
52	β -endorphin		ssNMR	6tub		28/10/2020	[137]
53	β 2m		cryo-EM		0019	19/06/2019	[138]
54	β 2m		cryo-EM		0021	29/05/2019	
55	β 2m		cryo-EM	6gk3	0014	14/11/2018	
56	β 2m		ssNMR	2e8d		13/02/2007	[139]
57	CA150		ssNMR	2nnt		14/11/2006	[140]
58	FUS		ssNMR & cryo-EM	6xfm	21169	07/10/2020	[141]
59	Glucagon		ssNMR	6nzn		05/06/2019	[142]
60	HET-s		ssNMR	2mus, 2lbu		01/02/2017	[143,144]
61	HET-s		cryo-EM		2946	15/04/2015	[145]
62	HET-s		ssNMR	2kj3, 2mm		02/06/2010	[146,147]
63	hnRNPA1		cryo-EM	7bx7	30235	18/11/2020	[148]
64	hnRNPA2		cryo-EM	6wqk	21871	26/08/2020	[85]
65	IAPP		cryo-EM	6zrf	11380	30/09/2020	[53]
66	IAPP		cryo-EM	6zrq	11382	30/09/2020	
67	IAPP		cryo-EM	6zrr	11383	30/09/2020	
68	IAPP		cryo-EM	6vw2	21410	10/06/2020	[149]
69	IAPP		cryo-EM	6y1a	10669	04/03/2020	[150]
70	IAPP		cryo-EM		10670	04/03/2020	
71	IAPP		cryo-EM		10671	04/03/2020	

72	IG LC	AL cardiac tissue	cryo-EM	6z1o	11031	24/02/2021	[57]
73	IG LC	AL cardiac tissue	cryo-EM	6z1i	11030	24/02/2021	
74	IG LC	AL cardiac tissue	cryo-EM	6ic3	4452	03/04/2019	[98]
75	IG LC	AL cardiac tissue	cryo-EM	6hud	0274	27/03/2019	[99]
76	IG LC		cryo-EM		3986	28/02/2018	[151]
77	IG LC		cryo-EM		3987	28/02/2018	
78	IG LC		cryo-EM		3988	28/02/2018	
79	IG LC		cryo-EM		3989	28/02/2018	
80	IG LC		cryo-EM		3990	28/02/2018	
81	IG LC		cryo-EM		3991	28/02/2018	
82	IG LC		cryo-EM		3992	28/02/2018	
83	IG LC		cryo-EM		3993	28/02/2018	
84	IG LC		cryo-EM		3994	28/02/2018	
85	IG LC		cryo-EM		3128	18/05/2016	
86	Orb2	<i>D. melanogaster</i> brain	cryo-EM	6vps	21316	18/03/2020	[87]
87	PI3K		cryo-EM	6r4r	4727	28/08/2019	[153]
88	PrP		cryo-EM	6lni	0931	10/06/2020	[154]
89	PrP		cryo-EM	6uur	20900	15/04/2020	[155]
90	RIPK1/RIPK3		ssNMR	5v7z		28/03/2018	[156]
91	RIPK3		ssNMR	6jpd		28/10/2020	[157]
92	SAA	Murine liver	cryo-EM	6zch	11164	17/02/2021	[39]
93	SAA		cryo-EM	6zcg	11163	17/02/2021	
94	SAA		cryo-EM	6zcf	11162	17/02/2021	
95	SAA	Murine spleen	cryo-EM	6dso	8910	13/03/2019	[158]
96	SAA	Amyloidotic kidney	cryo-EM	6mst	9232	13/03/2019	
97	tau	CBD brain	cryo-EM	6vh7	21200	04/03/2020	[38]
98	tau	CBD brain	cryo-EM	6vha	21201	04/03/2020	
99	tau	AD brain	cryo-EM	6vhl	21207	04/03/2020	
100	tau	CBD brain	cryo-EM	6tjx	10514	05/02/2020	[14]
101	tau	CBD brain	cryo-EM	6tjo	10512	05/02/2020	
102	tau	CTE brain	cryo-EM	6nwp	0527	27/03/2019	[15]
103	tau	CTE brain	cryo-EM	6nwq	0528	27/03/2019	
104	tau		cryo-EM	6qjh	4563	20/02/2019	[101]
105	tau		cryo-EM	6qjm	4564	20/02/2019	
106	tau		cryo-EM	6qjp	4565	20/02/2019	
107	tau		cryo-EM	6qjq	4566	20/02/2019	
108	tau	AD brain	cryo-EM	6hre	0259	10/10/2018	[92]
109	tau	AD brain	cryo-EM	6hrf	0260	10/10/2018	
110	tau	Pick's disease brain	cryo-EM	6gx5	0077	12/09/2018	[91]

111	tau	Pick's disease brain	cryo-EM		0078	12/09/2018	
112	tau	AD brain	cryo-EM	5o3l	3741	26/07/2017	[13]
113	tau	AD brain	cryo-EM	5o3o	3742	26/07/2017	
114	tau	AD brain	cryo-EM	5o3t	3743	26/07/2017	
115	tau	AD brain	cryo-EM		3744	26/07/2017	
116	TDP-43		cryo-EM	7kwz	23059	24/02/2021	
117	TDP-43		cryo-EM	6n3a	9349	26/06/2019	[160]
118	TDP-43		cryo-EM	6n3b	9350	26/06/2019	
119	TDP-43		cryo-EM	6n3c	0334	26/06/2019	
120	TDP-43		cryo-EM	6n37	9339	26/06/2019	
121	TDP-43		cryo-EM	5w7v	8781	14/03/2018	[161]
122	TTR	ATTR heart	cryo-EM	6sdz	10150	13/11/2019	[162]
123	TTR		ssNMR	2m5n		17/07/2013	[54]
124	TTR		cryo-EM	2m5k	5590	03/04/2013	
125	TTR		cryo-EM	2m5m	2323	27/03/2013	
126	TTR		cryo-EM	3zpk	2324	27/03/2013	
127	TTR		ssNMR	1rvs		20/01/2004	[163]

1 *. Database entries are ordered alphabetically by their protein name. Entries of amyloid formed
2 from the same protein are ordered by release date from the newest to the oldest. Where several
3 models have been published based on reanalysis of the same original data, the entries are
4 grouped and all accession codes are included in the same row.

5 §. The origin of the tissue from which *ex vivo* fibrils were extracted is noted. Where the species
6 is not specified, the tissue is of human origin, with the following abbreviations for disease
7 diagnoses: AD – Alzheimer's Disease, MSA – multiple system atrophy, CBD – corticobasal
8 degeneration, CTE – chronic traumatic encephalopathy, ATTR – transthyretin amyloidosis

9 †. The Protein Data Bank (PDB) ID code associated with the structural model.

10 ‡. The Electron Microscopy Data Bank (EMDB) accession codes associated with the EM
11 density map.

12